

Dual PPAR α / γ activation inhibits SIRT1-PGC1 α axis and causes cardiac dysfunction

Charikleia Kalliora,^{1,2} Ioannis D. Kyriazis,¹ Shin-ichi Oka,³ Melissa J. Lieu,¹ Yujia Yue,¹ Estela Area-Gomez,⁴ Christine J. Pol,¹ Ying Tian,¹ Wataru Mizushima,³ Adave Chin,³ Diego Scerbo,^{5,6} P. Christian Schulze,⁷ Mete Civelek,⁸ Junichi Sadoshima,³ Muniswamy Madesh,¹ Ira J. Goldberg,⁵ and Konstantinos Drosatos¹

¹Center for Translational Medicine, Department of Pharmacology, Lewis Katz School of Medicine at Temple University, Philadelphia, Pennsylvania, USA. ²Faculty of Medicine, University of Crete, Voutes, Greece. ³Cardiovascular Research Institute, Department of Cell Biology and Molecular Medicine, Rutgers New Jersey Medical School, Newark, New Jersey, USA. ⁴Department of Neurology, Columbia University Irving Medical Center, New York, New York, USA. ⁵Division of Preventive Medicine and Nutrition, Columbia University, New York, New York, USA. ⁶NYU Langone School of Medicine, Division of Endocrinology, Diabetes and Metabolism, New York, New York, USA. ⁷Department of Internal Medicine I, Division of Cardiology, Angiology, Intensive Medical Care and Pneumology, University Hospital Jena, Jena, Germany. ⁸Center for Public Health Genomics, Department of Biomedical Engineering, University of Virginia, Charlottesville, Virginia, USA.

Dual PPAR α / γ agonists that were developed to target hyperlipidemia and hyperglycemia in patients with type 2 diabetes caused cardiac dysfunction or other adverse effects. We studied the mechanisms that underlie the cardiotoxic effects of a dual PPAR α / γ agonist, tesaglitazar, in wild-type and diabetic (leptin receptor-deficient, *db/db*) mice. Mice treated with tesaglitazar-containing chow or high-fat diet developed cardiac dysfunction despite lower plasma triglycerides and glucose levels. Expression of cardiac PPAR γ coactivator 1- α (PGC1 α), which promotes mitochondrial biogenesis, had the most profound reduction among various fatty acid metabolism genes. Furthermore, we observed increased acetylation of PGC1 α , which suggests PGC1 α inhibition and lowered sirtuin 1 (SIRT1) expression. This change was associated with lower mitochondrial abundance. Combined pharmacological activation of PPAR α and PPAR γ in C57BL/6 mice reproduced the reduction of PGC1 α expression and mitochondrial abundance. Resveratrol-mediated SIRT1 activation attenuated tesaglitazar-induced cardiac dysfunction and corrected myocardial mitochondrial respiration in C57BL/6 and diabetic mice but not in cardiomyocyte-specific *Sirt1*^{-/-} mice. Our data show that drugs that activate both PPAR α and PPAR γ lead to cardiac dysfunction associated with PGC1 α suppression and lower mitochondrial abundance, likely due to competition between these 2 transcription factors.

Authorship note: CK and IDK contributed equally to this work.

Conflict of interest: The authors have declared that no conflict of interest exists.

Copyright: © 2019 American Society for Clinical Investigation

Submitted: April 12, 2019

Accepted: August 6, 2019

Published: September 5, 2019.

Reference information: *JCI Insight*. 2019;4(17):e129556. <https://doi.org/10.1172/jci.insight.129556>.

Introduction

Aside from improvement in hyperglycemia, various new therapies for treatment of type 2 diabetes focus on the effect of the new drugs on cardiovascular disease. Agonists of PPAR α and PPAR γ have been developed for the treatment of hyperlipidemia and hyperglycemia, respectively, based on their effects in reducing circulating triglyceride levels and promoting insulin sensitization.

PPARs belong to the nuclear receptors superfamily and promote fatty acid (FA) metabolism. PPAR α ligands, such as fibrates, lower plasma triglyceride levels and increase high-density lipoprotein-cholesterol levels (1). Thiazolidinediones (TZDs) are PPAR γ ligands and act as insulin sensitizers that lower plasma glucose (2). However, PPAR γ agonists have toxicity and can produce heart failure either due to direct actions on the heart or due to increased salt and water retention (3). Dual PPAR α / γ agonists (glitazars) were developed to combine the beneficial effects of PPAR α and PPAR γ agonism. Although these dual agonists improve metabolic parameters (4), some of them, such as tesaglitazar (5) and muraglitazar (6) were abandoned when clinical trials showed either increased risk for cardiovascular events or other adverse effects, such as increased peripheral edema and creatine phosphokinase via mechanisms that remain unknown.

PPARs are central regulators of cardiac FA metabolism (7). Cardiac PPAR α induces the expression of genes that orchestrate FA oxidation (FAO) and uptake (8). Greater FAO leads indirectly to lower cardiac glucose utilization (9). PPAR γ can also promote cardiac FAO (10, 11) when PPAR α expression is reduced (12) or ablated (11). Thus, both PPAR α and PPAR γ can orchestrate the cardiac FAO-related gene expression program. Because different PPAR isoforms can activate the same FA metabolism-related genes, dominance of one PPAR isoform over the other in controlling FA metabolism in a tissue depends on the abundance of the respective isoform as well as on the availability of endogenous isoform-specific ligands. FAO accounts for 70% of the ATP that is produced in the heart (13). Thus, it is surprising that combined activation of 2 positive regulators of cardiac FAO, PPAR α and PPAR γ , causes cardiac dysfunction.

PPAR γ coactivator 1- α (PGC1 α) is encoded by the *Ppargc1a* gene. It is the common transcriptional coactivator of PPAR α and PPAR γ and regulates cardiac FAO, mitochondrial biogenesis, and respiration (14). PGC1 α activation is controlled through reversible lysine side chain hyperacetylation that is attenuated by the enzymatic activity of the deacetylase sirtuin 1 (SIRT1) (15). SIRT1s are class III histone deacetylases activated by NAD⁺. Thus, they act as metabolic sensors of fluctuations in the NAD⁺/NADH ratio (16).

In this study, we investigated the effect of combined PPAR α / γ activation on PGC1 α expression and activation. Subsequently, we assessed whether the inhibitory effect of dual PPAR α / γ activation on PGC1 α activity is driven by downregulation of SIRT1. Our data show that cardiac dysfunction caused by an anti-diabetic dual PPAR α / γ agonist, tesaglitazar, is associated with reduced PGC1 α expression and activation (17–19). These effects are associated with competition between PPAR α and PPAR γ for regulation of *Ppargc1a* gene expression as well as by decreased cardiac SIRT1 expression. Activation of SIRT1 with resveratrol attenuated tesaglitazar-mediated cardiac dysfunction in C57BL/6 wild-type mice and in diabetic *db/db* (leptin receptor-deficient) mice but not in mice with cardiomyocyte-specific ablation of SIRT1. Our data elucidate the mechanism that underlies dual PPAR α / γ activation cardiotoxicity and identify a potentially new pharmacologic approach to prevent these side effects.

Results

Tesaglitazar causes cardiac dysfunction. Six-week-old C57BL/6 male mice were fed standard diet (chow) supplemented with tesaglitazar for 6 weeks. Tesaglitazar feeding did not alter plasma triglycerides or glucose levels (Figure 1, A and B) and neither did it affect weight gain rate and food consumption compared with respective controls (Supplemental Figure 1, A and B; supplemental material available online with this article; <https://doi.org/10.1172/jci.insight.129556DS1>). On the other hand, 2D echocardiography revealed that mice fed with tesaglitazar developed cardiac dysfunction (Figure 1, C and D). Specifically, tesaglitazar reduced left ventricular fractional shortening (FS%) by approximately 20% and increased left ventricular internal diameter during systole by 30% compared with chow-fed mice (Figure 1D and Supplemental Table 1).

Tesaglitazar-mediated cardiac dysfunction is associated with lower PGC1 α protein levels. Because tesaglitazar is a dual agonist for both PPAR α and PPAR γ , we examined expression of cardiac FAO-genes in mice treated with tesaglitazar. The expression of *Ppargc1a*, which encodes for the common transcriptional coactivator of PPARs (20) and promotes mitochondrial biogenesis, showed a strong trend ($P = 0.104$) for reduction (20%) at the mRNA level (Figure 1E) and clear reduction (~45%) at the protein level (Figure 1F). Among several FA metabolism-related genes, *Ppard* expression was increased by 2.6-fold and uncoupling protein 3 (*Ucp3*) expression had a strong trend of increase (87%; Figure 1G). In contrast to these changes, cardiac PPAR α and PPAR γ protein levels were not significantly altered in tesaglitazar-treated mice (Supplemental Figure 1, C and D).

PPAR α activation compromised PPAR γ -mediated induction of PGC1 α . To test whether the effect of tesaglitazar on PGC1 α levels relies on combined activation of PPAR α and PPAR γ , we tested whether individual PPAR α and PPAR γ activation by their respective ligands has a similar effect. First, we performed dose-titration experiments to identify the minimum dose of rosiglitazone (PPAR γ agonist) that increases cardiac *Ppargc1a* expression levels and the maximum dose of WY-14643 (PPAR α agonist) that does not affect it. Specifically, we administered a series of doses of rosiglitazone or WY-14643 (25 mg/kg body weight, 12.5 mg/kg body weight, 6.25 mg/kg body weight, 3.125 mg/kg body weight) via i.p. injections in C57BL/6 mice. This experiment showed that 25 mg/kg body weight was the lowest dose of rosiglitazone that induced cardiac *Ppargc1a* expression (Figure 2A) and 12.5 mg/kg body weight was the highest dose of WY-14643 that did not (Figure 2A). C57BL/6 mice were then injected with a combination of 25 mg/kg body weight rosiglitazone and 12.5 mg/kg body weight WY-14643. The combined treatment prevented rosiglitazone-mediated upregulation of cardiac *Ppargc1a* gene expression (Figure 2A). Accordingly,

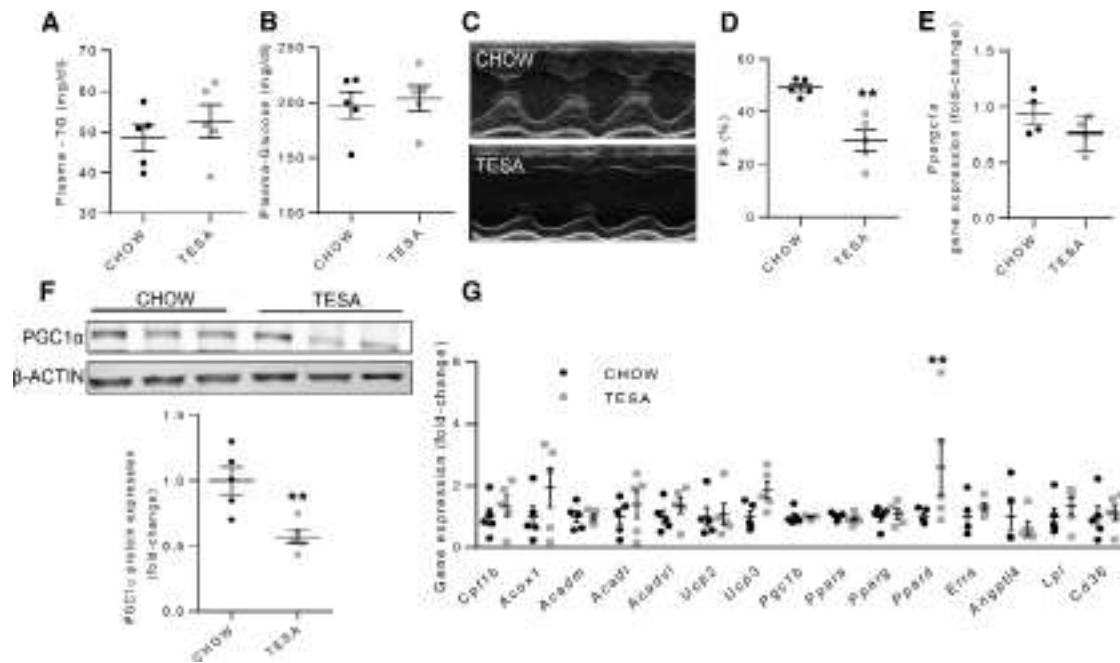


Figure 1. Tesaglitazar causes cardiac dysfunction. C57BL/6 mice were treated with control chow or tesaglitazar-containing (TESA-containing) chow (0.5 $\mu\text{mol/kg}$ bw) for 6 weeks (all mice were treated in 1 experiment). After termination of treatment, plasma triglycerides (TG, **A**; $n = 5$) and plasma glucose (**B**; $n = 5$) were assessed. Cardiac function was determined and is represented here with short-axis M-mode echocardiography images (**C**) and calculation of left ventricular fractional shortening (**D**; $n = 5$). After the treatment period, cardiac PPAR γ coactivator 1 α (*Ppargc1a*) mRNA levels (**E**; $n = 4$) and the respective protein levels (PGC1 α) were assessed (**F**; representative immunoblot and densitometric analysis normalized to β -ACTIN; $n = 5$). (**G**) Cardiac carnitine palmitoyltransferase 1- β (*Cpt1b*), acyl-CoA oxidase 1 (*Acox1*), medium-chain acyl-CoA dehydrogenase (*Acadm*), long-chain acyl-CoA dehydrogenase (*Acadl*), very-long-chain acyl-CoA dehydrogenase (*Acadvl*), uncoupling protein 2 (*Ucp2*), *Ucp3*, *Ppargc1b*, *Ppara*, *Pparg*, *Ppard*, estrogen-related receptor α (*Erra*), angiotensin-like-4 (*Angptl4*), lipoprotein lipase (*Lpl*), and cluster of differentiation 36 (*Cd36*) mRNA levels were assessed (**G**; $n = 5$). Statistical analysis was performed using unpaired 2-tailed Student's *t* test. ** $P < 0.01$. Error bars represent SEM.

combined administration of rosiglitazone and WY-14643 prevented PPAR γ -mediated upregulation of the expression of lipid uptake-related genes, such as cluster of differentiation 36 (*Cd36*) and *Lpl* (Figure 2B). Rosiglitazone also increased *CPT1B* (2.3-fold) and *ACOX1* (2.5-fold) mRNA levels, but combined injection of both PPAR α and PPAR γ agonists in C57BL/6 mice blocked the effects of rosiglitazone (Figure 2C). Conversely, PPAR α and PPAR γ did not seem to compete for regulation of other genes. Specifically, treatment of C57BL/6 mice with WY-14643 did not prevent a rosiglitazone-mediated trend of increase of *Acadl* (~25-fold) gene expression (Figure 2C). Cardiac *Ucp3* gene expression was increased (3.2-fold) by WY-14643 and retained the same levels in mice treated with the combination (Figure 2C). On the other hand, both individual agonist treatments, as well as combined administration, increased the expression of *Angptl4* with rosiglitazone being the major inducer (single treatment: 35-fold and combined treatment: strong trend of 25-fold increase) compared with WY-14643 single treatment (2.5-fold) (Figure 2B). Thus, although combined PPAR α / γ activation led to greater expression of some FAO-related genes, the expression of *Ppargc1a* and some other downstream PPAR targets was not increased.

Combined PPAR α / γ activation decreased cardiac mitochondrial abundance and respiration. PGC1 α promotes mitochondrial biogenesis (14) by controlling the expression of mitochondrial transcription factor A (mtTFA, encoded by *Tfam* gene) (21). Given that combined administration of single PPAR α and PPAR γ agonists prevented rosiglitazone-mediated upregulation of PGC1 α , and treatment with the dual PPAR α / γ agonist, tesaglitazar, had an inhibitory effect on cardiac PGC1 α levels, we tested whether combined PPAR α and PPAR γ activation affects mitochondrial abundance and function. Cardiac *TFAM* mRNA levels were increased (2-fold) in rosiglitazone-treated C57BL/6 mice, but combined treatment with rosiglitazone and WY-14643 prevented this increase (Figure 3A). Conversely, hearts from mice treated with the combination of rosiglitazone and WY-14643 exhibited a reduced mitochondrial DNA (mtDNA) to nuclear DNA (nuDNA) ratio (–31%; Figure 3B), demonstrating that combined activation of PPAR α and PPAR γ prevents rosiglitazone-mediated increased expression of PGC1 α and reduces mitochondrial abundance.

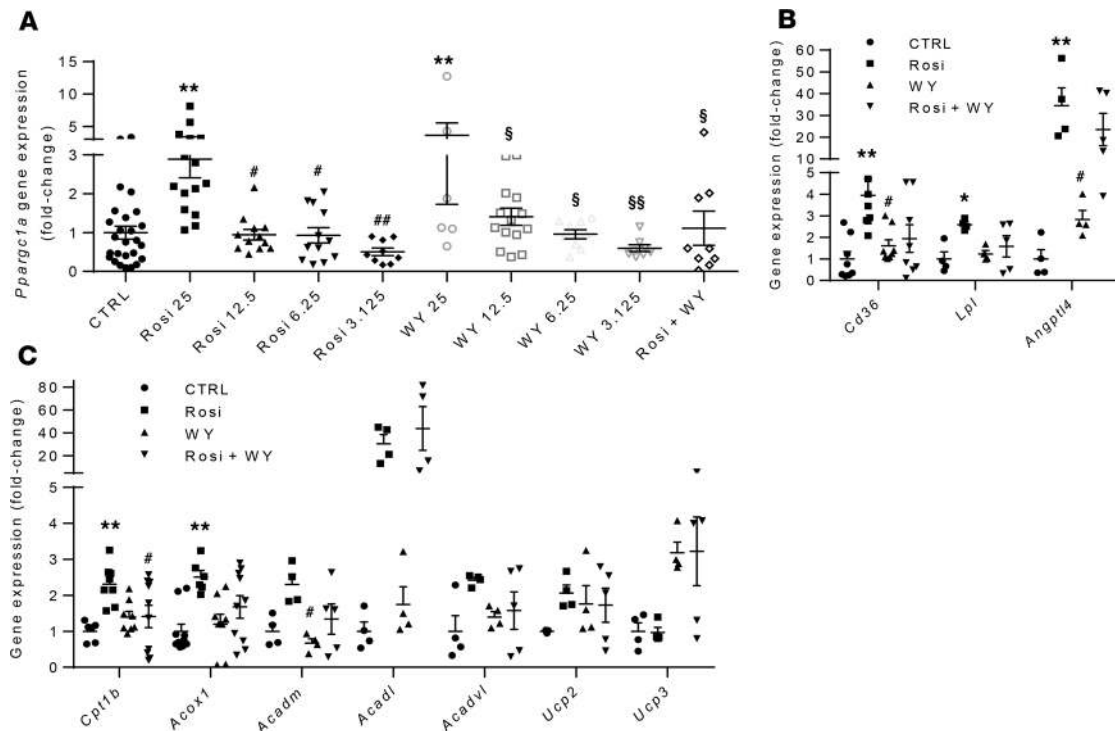


Figure 2. PPAR α interferes with PPAR γ -mediated induction of tesaglitazar on *Pparg1a* expression. (A) C57BL/6 mice injected i.p. with 25, 12.5, 6.25, and 3.125 mg/kg of body weight (bw) rosiglitazone (PPAR γ agonist) and 3.125 mg/kg bw WY-14643 (PPAR α agonist) or a combination of rosiglitazone (25 mg/kg bw) and WY-14643 (12.5 mg/kg bw) to assess the cardiac PPAR γ coactivator 1- α (*Pparg1a*) mRNA levels ($n = 6-16$). Control (CTRL) mice ($n = 26$) received DMSO. (B and C) C57BL/6 mice were treated i.p. with rosiglitazone (25 mg/kg bw), WY-14643 (12.5 mg/kg bw), or a combination of rosiglitazone (25 mg/kg bw) and WY-14643 (12.5 mg/kg bw) and cardiac cluster of differentiation (*Cd36*), lipoprotein lipase (*Lpl*), and angiopoietin like-4 (*Angptl4*) (B; $n = 4-8$) and carnitine palmitoyltransferase 1- β (*Cpt1b*), acyl-CoA oxidase 1 (*Acox1*), medium-chain acyl-CoA dehydrogenase (*Acadm*), long-chain acyl-CoA dehydrogenase (*Acadl*), very-long-chain acyl-CoA dehydrogenase (*Acadvl*), uncoupling protein 2 (*Ucp2*), and *Ucp3* (C; $n = 4-10$) mRNA levels were assessed. Control mice were treated with DMSO. Statistical analyses were performed with 1-way ANOVA followed by Tukey's correction. Error bars represent SEM. * $P < 0.05$ vs. CTRL; ** $P < 0.01$ vs. CTRL. # $P < 0.05$ vs. rosiglitazone (25 mg/kg bw); ## $P < 0.01$ vs. rosiglitazone (25 mg/kg bw). \$ $P < 0.05$ vs. WY-14643 (25 mg/kg bw); \$\$ $P < 0.01$ vs. WY-14643 (25 mg/kg bw). The data presented here were collected from 2-3 independent experiments.

In accordance with the previous finding, mitochondrial MitoTracker Red staining (Figure 3, C and D) of primary adult cardiomyocytes (ACMs) isolated from mice subjected to daily i.p. injections with tesaglitazar (2 mg/kg body weight) for 7 days showed lower mitochondrial abundance (-67% ; Figure 3D) compared with the ACMs derived from control mice (DMSO injected). Accordingly, a human cardiomyocyte cell line (AC16) (22) that was treated with tesaglitazar (50 μ M and 100 μ M) for 24 hours showed decreased mitochondrial abundance (-42% for cells treated with 100 μ M tesaglitazar) (Supplemental Figure 2, A and B).

In order to assess whether the reduction in mitochondrial number affected respiratory capacity of cardiomyocytes, we measured oxygen consumption rate (OCR) using the Seahorse Bioscience XF96 Analyzer in primary ACMs derived from mice that were treated with tesaglitazar. This analysis showed impaired mitochondrial respiration, as shown by lower basal respiration, maximal respiration, and spare respiratory capacity (Figure 3, E and F).

*PPAR α and PPAR γ compete for the regulation of the *Pparg1a* promoter.* In order to confirm that the lack of induction of *Pparg1a* gene expression upon combined pharmacologic PPAR α and PPAR γ activation of is not accounted for by off-target effects of rosiglitazone and WY-14643, we infected AC16 cells with recombinant adenoviruses expressing human PPAR α (Ad-PPAR α) and PPAR γ (Ad-PPAR γ). Similar to that seen with pharmacologic activation of PPAR α and PPAR γ , *PPARGCIA* mRNA levels were increased (2.6-fold) in cells treated with Ad-PPAR γ (Figure 4A). The positive effect of PPAR γ on *PPARGCIA* gene expression was blocked in cells infected with a combination of Ad-PPAR α and Ad-PPAR γ (Figure 4A).

Next, we treated AC16 cells with increasing doses of rosiglitazone (25, 50, and 100 μ M) and WY-14643 (25, 50, and 100 μ M) to identify the minimum dose of rosiglitazone that increases *PPARGCIA* expression (Supplemental Figure 3, A-C) and the maximum dose of WY-14643 that does not (Supplemental Figure 3, D-F).

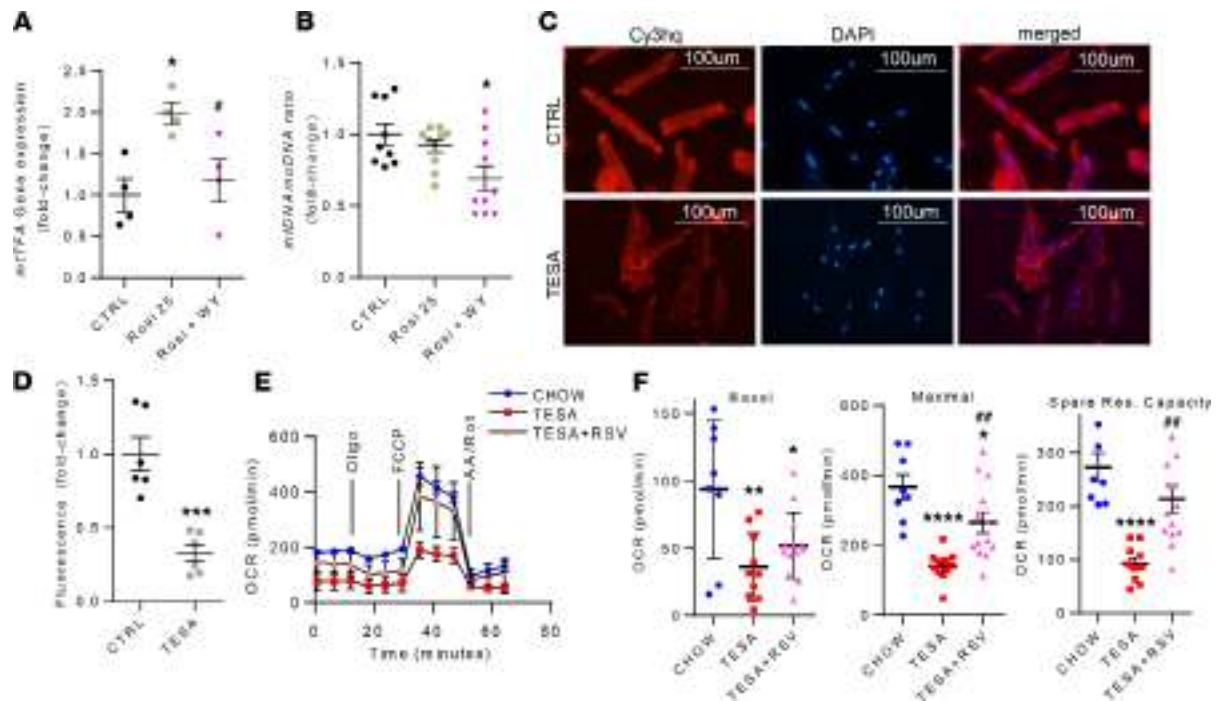


Figure 3. Tesaglitazar reduces mitochondrial abundance in cardiomyocytes. (A and B) C57BL/6 mice were injected i.p. with rosiglitazone (PPAR γ agonist; 25 mg/kg bw), WY-14643 (PPAR α agonist; 12.5 mg/kg bw), or a combination of rosiglitazone (25 mg/kg bw) and WY-14643 (12.5 mg/kg bw). Cardiac mitochondrial transcription factor A (TFAM) mRNA levels (A; $n = 4$) and mitochondrial abundance were determined by measuring the mitochondrial DNA (mtDNA) to nuclear DNA (nuDNA) ratio (fold change) (B; $n = 9-10$). Control (CTRL) mice were treated with DMSO. (C and D) C57BL/6 mice were subjected to daily i.p. injections with tesaglitazar (TESA) (2 mg/kg bw) for 7 days, and primary adult cardiomyocytes (ACMs) were isolated. Representative images (C, original magnification, $\times 20$; scale bar: 100 μm) obtained from fluorescence microscopy of isolated ACMs stained with MitoTracker Red and mitochondrial number/total area were quantified (D) ($n = 6$, number of analyzed cells: control, 127; tesaglitazar, 125; data derived from 3 independent experiments). (E and F) ACMs were isolated from C57BL/6 mice upon completion of 6 weeks feeding on regular chow, chow diet containing tesaglitazar (0.5 $\mu\text{mol/kg}$ body weight), or chow with combination of tesaglitazar (0.5 $\mu\text{mol/kg}$ body weight) and resveratrol (RSV; 100 mg/kg body weight/day). Oxygen consumption rate (OCR; E) and basal respiration, maximal respiration, and spare respiratory capacity (F) measured with XF96 Seahorse Analyzer. Oligo, oligomycin (3 μM); FCCP, carbonyl cyanide-p-trifluoromethoxyphenylhydrazone (2 μM); AA/Rot, antimycin a/rotenone (0.5 μM) ($n = 8-13$ wells with ACMs isolated from 3 individual mice per experimental group). Statistical analyses for all graphs were performed with 1-way ANOVA followed by Tukey's correction except D, which was analyzed with an unpaired 2-tailed Student's t test. * $P < 0.05$; ** $P < 0.01$; *** $P < 0.001$; **** $P < 0.0001$ vs. CTRL or chow. # $P < 0.05$; ## $P < 0.01$ vs. rosiglitazone 25 or tesaglitazar. Error bars represent SEM. * indicates statistical difference with control chow, # indicates difference with rosiglitazone- or tesaglitazar-treated mice.

This analysis prompted us to select 50 μM rosiglitazone and 50 μM WY-14643 for further in vitro experiments. Treatment of AC16 cells with 50 μM rosiglitazone increased *PPARGC1A* mRNA levels (3.34-fold) (Figure 4B). The same dose, however, did not increase *PPARGC1A* mRNA levels after combination with 50 μM WY-14643 (Figure 4B). The inhibitory effect of WY-14643 on the rosiglitazone-mediated increase of *PPARGC1A* mRNA levels was partially abolished upon coadministration of 10 μM MK886, a PPAR α antagonist (Figure 4B).

As both adenovirus-mediated and combined pharmacological PPAR α and PPAR γ agonists suppressed PPAR γ -mediated upregulation of *PPARGC1A* expression, we tested whether this effect was driven by altered *PPARGC1A* promoter activity. We first tested whether human *PPARGC1A* promoter (obtained from UCSC Genome Browser) contains PPAR response elements (PPREs). Analysis of the *PPARGC1A* promoter sequence up to 2,000 bp before the transcription initiation site (Genomatix) and sequence comparison between the human and murine *PPARGC1A* promoter sequence (CLUSTAL O 1.2.0 sequence alignment software) (Supplemental Figure 4A) identified 5 conserved PPREs that span regions -1631/-1609 bp, -1386/-1362 bp, -1012/-991 bp, -634/-612 bp, and -210/-189 bp (Supplemental Figure 4B). To map the region of the human *PPARGC1A* promoter that is responsible for the inhibitory effect of PPAR α on PPAR γ -mediated upregulation of *PPARGC1A* expression, we generated a panel of *PPARGC1A* promoter deletion mutants (Supplemental Figure 4C) and cloned this panel into the pGL3-BV luciferase reporter plasmid. We transfected AC16 cells with reporter plasmids containing *PPARGC1A* promoter deletion mutants, pGL3BV-*PPARGC1A*-1631, pGL3BV-*PPARGC1A*-1386, pGL3BV-*PPARGC1A*-1012, and pGL3BV-*PPARGC1A*-210, and treated them with 50 μM rosiglitazone, 50 μM WY-14643, or a combination of both. Rosiglitazone increased luciferase activity of

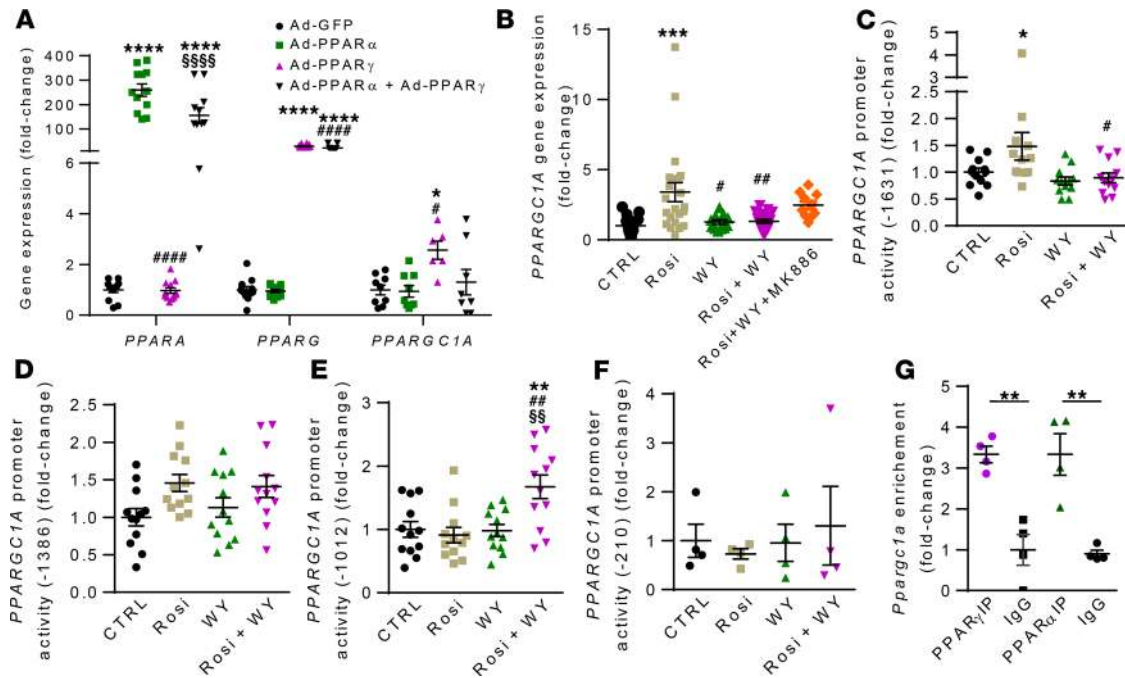


Figure 4. PPAR α impairs PPAR γ -mediated activation of PPARGC1A promoter activity. (A) PPAR α , PPARG, and PPARGC1A mRNA levels were assessed in AC16 cells infected with recombinant adenoviruses (Ad) expressing PPAR α or PPAR γ ($n = 6$ –12; data were collected from 2 independent experiments). * $P < 0.05$; **** $P < 0.0001$ vs. Ad-GFP; # $P < 0.05$; ##### $P < 0.0001$ vs. Ad-PPAR α ; \$\$\$ $P < 0.0001$ vs. Ad-PPAR γ . (B) Ppargc1a mRNA levels in AC16 cells treated with 50 μ M rosiglitazone (PPAR γ agonist), 50 μ M WY-14643 (PPAR α agonist), a combination of rosiglitazone and WY-14643, or a combination of rosiglitazone, WY-14643, and 10 μ M MK886 (PPAR α antagonist) (B; $n = 10$ –22; data were collected from 2 independent experiments). (C–F) Luciferase activity (fold change) in AC16 cells transfected with reporter plasmids containing the following human PPAR γ coactivator 1- α (PPARGC1A) promoter fragments: pGL3-basic vector(BV)-PPARGC1A-1631 (C), pGL3BV-a-PPARGC1A-1386 (D), pGL3BV-a-PPARGC1A-1012 (E), pGL3BV-a-PPARGC1A-210 (F), followed by treatment with 50 μ M rosiglitazone, 50 μ M WY-14643, or a combination of both ($n = 4$ –12). (B–F) Data were collected from 1 experiment. * $P < 0.05$; ** $P < 0.01$; *** $P < 0.001$ vs. ctrl; # $P < 0.05$; ## $P < 0.01$ vs. rosiglitazone; \$\$\$ $P < 0.01$ vs. WY-14642. (G) PPAR α and PPAR γ enrichment of the Ppargc1a gene promoter following chromatin immunoprecipitation from cardiac tissue obtained from C57BL/6 mice ($n = 4$). *** $P < 0.01$. Statistical analyses were performed with 1-way ANOVA followed by Tukey's post hoc correction. Error bars represent SEM.

pGL3BV-PPARGC1A-1631 (Figure 4C), while it did not have any effect on pGL3BV-PPARGC1A-1386 (Figure 4D), pGL3BV-PPARGC1A-1012 (Figure 4E), and pGL3BV-PPARGC1A-210 (Figure 4F). On the other hand, WY-14643 did not increase luciferase activity in any of the groups (Figure 4, C–F). However, the combined treatment with rosiglitazone and WY-14643 prevented a rosiglitazone-mediated increase in the activity of the PPARGC1A-1631 promoter fragment (Figure 4C). Thus, PPAR α and PPAR γ compete for regulation of PPARGC1A gene expression and activation of PPAR α prevents PPAR γ -mediated induction of PPARGC1A promoter activity when the PPRE of the –1631/–1609 bp region is present.

Our *in silico* analysis predicted a flanking region of –1631/–1609 bp in the PPARGC1A gene promoter (Supplemental Figure 4A). In order to assess binding capacity of PPAR α and PPAR γ on this region, we performed chromatin immunoprecipitation assays using homogenates of hearts from C57BL/6 mice. Significant enrichment of both PPAR α and PPAR γ was observed in the Ppargc1a gene promoter (Figure 4G). These results suggest that PPAR α and PPAR γ can bind to the identical PPRE and, therefore, may compete for binding.

Tesaglitazar-decreased cardiac SIRT1 expression and increased PGC1 α acetylation. PGC1 α activation is controlled via deacetylation of lysine residues by the deacetylase SIRT1 (15). Thus, we determined whether tesaglitazar-mediated cardiac dysfunction is also associated with altered acetylation of PGC1 α . Acetylated PGC1 α (Ac-PGC1 α) that was normalized to heavy IgG and PGC1 α input was increased in hearts of mice fed with tesaglitazar-containing chow (2.5-fold; Figure 5A and Supplemental Figure 5A). In accordance with the increased Ac-PGC1 α levels, SIRT1 protein levels were decreased in tesaglitazar-treated mice (~30%; Figure 5B and Supplemental Figure 5B).

To verify that the cardiac SIRT1 decrease was cardiomyocyte-specific, we isolated ACMs from mice that had undergone daily *i.p.* injections with tesaglitazar (2 mg/kg body weight) for 7 days. SIRT1 protein levels were decreased by 58% in ACMs derived from tesaglitazar-injected mice (Figure 5, C and D).

Tesaglitazar treatment did not change Pparg1a and SIRT1 expression in Ppara^{-/-} mice. In order to further test whether combined PPAR α and PPAR γ activation accounts for the cardiotoxic effects of tesaglitazar, we treated *Ppara^{-/-}* mice with chow diet enriched with tesaglitazar for 6 weeks. The effect of tesaglitazar on cardiac function was less substantially in mice with PPAR α ablation (Figure 5, E and F) compared with C57BL/6 mice (Figure 1, C and D). In addition, tesaglitazar treatment of *Ppara^{-/-}* mice did not suppress cardiac PGC1 α (Figure 5, G and H) and SIRT1 protein (Figure 5, G and I). The mild decrease in cardiac function of the tesaglitazar-treated *Ppara^{-/-}* mice was associated with increased cardiac expression of *Nppb* (encodes brain natriuretic peptide 4.2-fold) and *Col1a1* (encodes collagen, type I, α 1; 37-fold) gene expression (Figure 5J). Tesaglitazar-treated *Ppara^{-/-}* mice had increased *Pparg* expression (13-fold) as well as increased *Angptl4*, *Lpl*, *Acox1*, and *Cpt1b* expression (Figure 5J). Cardiac expression of *Ucp2*, *Ucp3*, *LpL*, *Acta1* (encodes skeletal α -actin), and *Nppa* (encodes atrial natriuretic peptide) were not significantly affected (Figure 5J). In addition, *Ppara* ablation was associated with a 5-fold increase in the cardiac mtDNA/nuDNA ratio in tesaglitazar-treated mice (Figure 5K).

Resveratrol ameliorated cardiotoxicity of tesaglitazar and maintained its beneficial effects. As tesaglitazar decreased SIRT1 expression and increased Ac-PGC1 α levels, we assessed whether pharmacological activation of SIRT1 by resveratrol and eventually PGC1 α would alleviate cardiac toxicity driven by dual PPAR α/γ activation. Thus, we treated C57BL/6 mice with chow diet containing tesaglitazar (0.5 μ mol/kg body weight) or a combination of tesaglitazar (0.5 μ mol/kg body weight) and resveratrol (100 mg/kg body weight/day; refs. 23, 24) for 6 weeks. We did not observe any effect of tesaglitazar alone or in combination with resveratrol in the weight gain rate (Supplemental Figure 6), plasma glucose (Figure 6A), or triglyceride (Figure 6B) levels. Analysis with 2D echocardiography confirmed a significant cardiac dysfunction in mice treated with tesaglitazar for 6 weeks (Figure 6, C and D, and Supplemental Table 2). However, mice treated with a combination of tesaglitazar and resveratrol showed significant improvement in cardiac function (FS%) compared with mice treated with tesaglitazar alone (Figure 6, C and D, and Supplemental Table 2). These findings showed that resveratrol attenuated the tesaglitazar-mediated cardiac dysfunction in C57BL/6 wild-type mice. No significant difference was observed in gene expression of markers for cardiac dysfunction or hypertrophy, such as *Nppb* and *Acta1* among all treatment groups (Supplemental Figure 7).

We then tested whether resveratrol-mediated improvement of cardiac function was accompanied by altered cardiac PGC1 α activation. Combined treatment of tesaglitazar with resveratrol decreased Ac-PGC1 α levels that were elevated in tesaglitazar-fed mice (Figure 6E and Supplemental Figure 5A). Combined tesaglitazar and resveratrol treatment increased SIRT1 protein levels (58%) compared with tesaglitazar-fed mice (Figure 6F and Supplemental Figure 5B). Moreover, mice fed on chow diet enriched with tesaglitazar and resveratrol exhibited increased cardiac SIRT3 protein levels (2.3-fold; Supplemental Figure 8, A and B) but not SIRT6 protein levels (Supplemental Figure 8, A and C).

Combined tesaglitazar and resveratrol treatment improved mitochondrial respiration. Analysis of mitochondrial respiration in isolated primary ACMs from C57BL/6 mice treated with chow diet enriched with tesaglitazar and resveratrol showed restoration of mitochondrial respiration compared with mice treated with tesaglitazar alone, as shown by improved maximal respiration and spare respiratory capacity (Figure 3, E and F). As alterations in OCR may correlate with differences in mitochondrial abundance, we performed MitoTracker staining in primary ACMs obtained from mice that received daily i.p. injections with tesaglitazar (2 mg/kg body weight/day) or a combination of tesaglitazar and resveratrol (100 mg/kg body weight/day) for 7 days (Figure 7A). ACMs obtained from mice treated with tesaglitazar alone showed a reduction (-67%) in mitochondrial abundance (Figure 7B). This effect did not occur in ACMs from mice treated with tesaglitazar and resveratrol (Figure 7B). Similarly, AC16 cells that were treated with tesaglitazar for 24 hours showed lower (-46%) mitochondrial abundance that did not occur following combined tesaglitazar and resveratrol treatment (Supplemental Figure 9, A and B). The mtDNA/nuDNA ratio exhibited a trend of reduction in hearts of tesaglitazar-treated mice (-20%), which did not occur in mice that were treated with combined tesaglitazar and resveratrol treatment (Figure 7C).

Mice treated with combination of resveratrol and tesaglitazar had a distinct cardiac lipidomic signature. As treatment with tesaglitazar reduced mitochondrial abundance and respiratory capacity, we tested whether it also affects cardiac lipid content. Lipidomic analysis revealed significant differences in most of the lipid classes we assessed. Heatmap analysis for the lipid species that we tested followed by hierarchical clustering of those that changed significantly indicated distinct cardiac lipidomic signatures among the 3 groups of mice (chow-fed control vs. tesaglitazar vs. tesaglitazar + resveratrol) (Figure 7D and Supplemental Table 3). Specifically, this analysis showed that tesaglitazar increased cardiac triglycerides (6.8-fold), acyl-carnitines (2.3-fold),

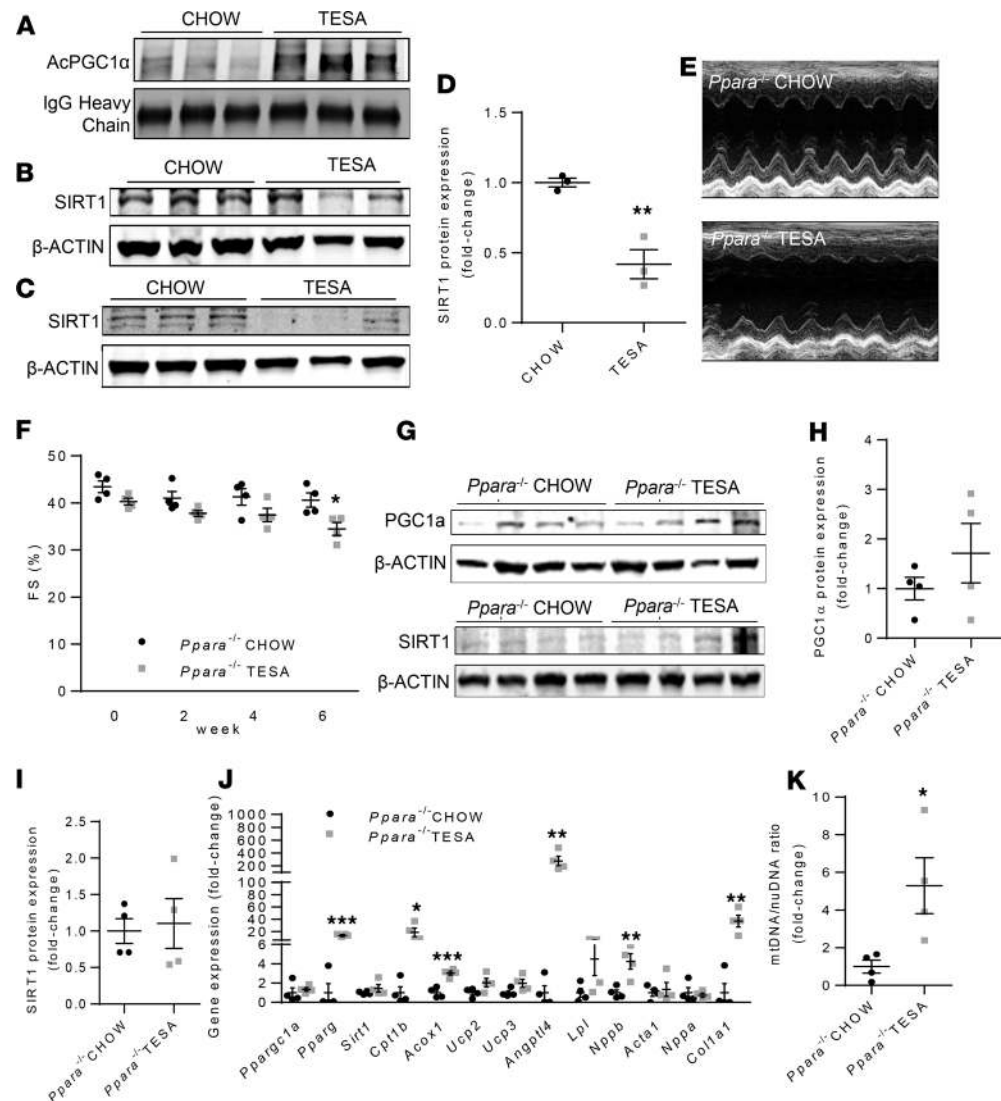


Figure 5. Tesaglitazar suppresses SIRT1 expression and promotes acetylation of PGC1 α . (A and B) Immunoblot of anti-PPAR γ coactivator 1- α (anti-PGC1 α) following immunoprecipitation with anti-Ac-lysine antibody of acetylated-PGC1 α (Ac-PGC1 α) and of the heavy IgG chain (A) and sirtuin 1 (SIRT1) and β -ACTIN protein levels (B) in hearts obtained from C57BL/6 mice fed on regular or tesaglitazar-containing chow (0.5 μ mol/kg bw) diet for 6 weeks (densitometric analysis is shown in Supplemental Figure 5, A and B; statistical analysis was performed for data collected from 2 independent experiments; $n = 8$). (C and D) Representative immunoblot and densitometric analysis of SIRT1 and β -ACTIN protein levels in ACMs isolated from C57BL/6 mice treated i.p. with tesaglitazar (2 mg/kg bw) for 7 days ($n = 3$; all data were collected from 1 experiment). (E and F) PPAR α -knockout mice (*Ppara*^{-/-}) were fed with regular or tesaglitazar-containing chow (0.5 μ mol/kg bw) diet for 6 weeks ($n = 4$; all data were collected from 1 experiment). Representative short-axis M-mode echocardiography images (E) and left ventricular fractional shortening (F) of *Ppara*^{-/-} mice treated with regular or tesaglitazar-containing chow for 6 weeks. (G–L) Representative immunoblots (G) and densitometric analysis of PGC1 α (G and H), SIRT1 (G and I), and β -ACTIN protein levels, cardiac *Ppargc1a*, *Pparg*, *Sirt1*, carnitine palmitoyltransferase 1- β (*Cpt1b*), acyl-CoA oxidase 1 (*Acox1*), uncoupling protein 2 (*Ucp2*), *Ucp3*, angiotensin-like-4 (*Angptl4*), lipoprotein lipase (*Lpl*), natriuretic peptide B (*Nppb*), actin α 1 (*Acta1*), natriuretic peptide type A (*Nppa*), and collagen type I α 1 chain (*Col1a1*) mRNA levels (J). Mitochondrial DNA (mtDNA) to nuclear DNA (nuDNA) ratio (K) in hearts obtained from *Ppara*^{-/-} mice fed on regular or tesaglitazar-containing chow (0.5 μ mol/kg bw) for 6 weeks ($n = 4$). Statistical analyses were performed with unpaired 2-tailed Student's t tests. * $P < 0.05$; ** $P < 0.01$; *** $P < 0.001$ vs. chow. Error bars represent SEM.

diacylglycerols (3.1-fold), and phosphatidic acid (30%). Tesaglitazar treatment reduced phosphatidylcholine (–37%), while there was a strong trend for reduction of monoacylglycerols (–40%) and ceramides (–27%). Combined treatment with tesaglitazar and resveratrol restored normal levels of acyl-carnitines, phosphatidic acid, phosphatidylcholine, monoacylglycerols, and ceramides (Supplemental Table 3).

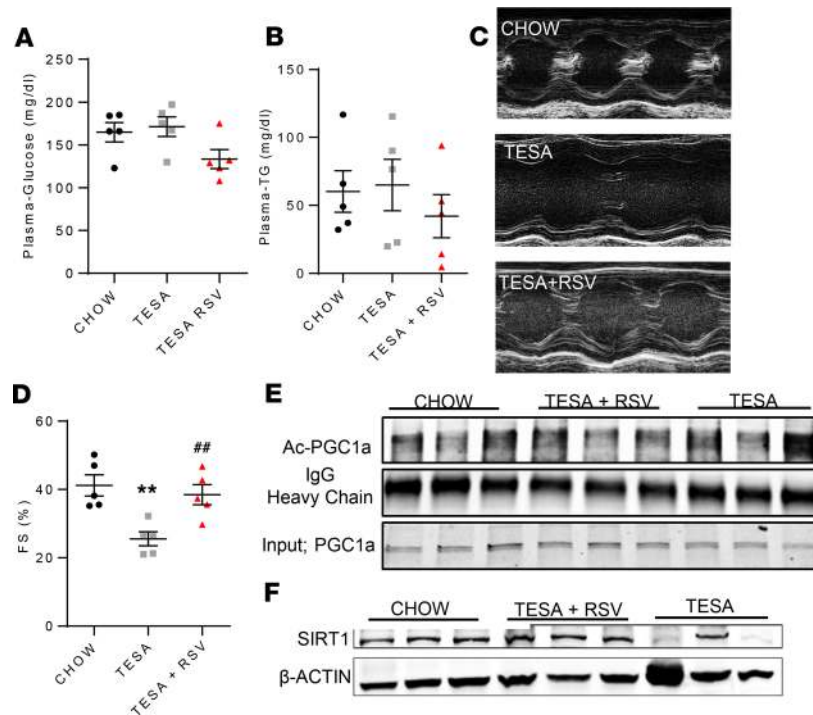


Figure 6. Resveratrol negates the cardiotoxic effect of tesaglitazar. (A–D) C57BL/6 mice were fed on chow containing tesaglitazar (0.5 $\mu\text{mol/kg}$ bw), combination of tesaglitazar (0.5 $\mu\text{mol/kg}$ bw) and resveratrol (RSV; 100 mg/kg bw/day), or regular chow for 6 weeks. Plasma glucose (A) and plasma triglycerides (TG) (B) were determined upon completion of the treatment. Representative short-axis M-mode echocardiography images (C; after treatment termination) and left ventricular fractional shortening (D) of C57BL/6 mice fed on chow containing tesaglitazar (0.5 $\mu\text{mol/kg}$ bw) or a combination of tesaglitazar (0.5 $\mu\text{mol/kg}$ bw) and RSV (100 mg/kg bw/day) for 6 weeks ($n = 5$; data were collected from 1 experiment). (E and F) Immunoblots of cardiac acetylated-PPAR γ coactivator 1- α (ac-PGC1 α) (E), IgG heavy chain, total PGC1 α , sirtuin 1 (SIRT1), and β -ACTIN (F) of C57BL/6 mice fed on regular chow or chow containing tesaglitazar (0.5 $\mu\text{mol/kg}$ bw) or a combination of tesaglitazar (0.5 $\mu\text{mol/kg}$ bw) and RSV (100 mg/kg bw/day) for 6 weeks (densitometric analysis is shown in Supplemental Figure 5, A and B; statistical analysis was performed for data collected from 2 independent experiments; $n = 5$ –8). Statistical analyses were performed with 1-way ANOVA followed by Tukey's post hoc correction among groups. ** $P < 0.01$ vs. chow; ## $P < 0.01$ vs. tesaglitazar. Error bars represent SEM.

Combined tesaglitazar and resveratrol treatment lowers plasma lipids and glucose without cardiotoxicity in diabetic and high-fat diet-fed mice. We next examined whether the combined treatment with tesaglitazar and resveratrol would exert its beneficial effect in a model of type 2 diabetes. Therefore, *db/db* mice were given chow diet containing no drugs, tesaglitazar, or a combination of tesaglitazar and resveratrol for 6 weeks. No significant effect was observed on weight gain rate between mice treated with tesaglitazar or tesaglitazar and resveratrol (Supplemental Figure 10A). Combined tesaglitazar and resveratrol treatment corrected hyperlipidemia (Figure 8A) and hyperglycemia (Figure 8B) to a similar extent to that of tesaglitazar alone. Despite the similar effect of tesaglitazar alone and tesaglitazar and resveratrol in combination in lowering plasma lipids and glucose, only the single tesaglitazar treatment caused cardiac dysfunction (Figure 8, C and D, and Supplemental Table 4). On the other hand, combined tesaglitazar and resveratrol treatment did not affect cardiac function (Figure 8, C and D) and neither did it modulate cardiac mitochondrial abundance (Figure 8E).

As in C57BL/6 mice, *db/db* mice that were fed on chow diet or diet containing a combination of tesaglitazar and resveratrol did not have the increase in PGC1 α acetylation that was observed in *db/db* mice treated with tesaglitazar alone (Figure 8, F and G). Changes in cardiac Ac-PGC1 α levels were accompanied by concomitant changes in cardiac SIRT1 protein levels, which were decreased (–39%) with tesaglitazar and restored to normal levels with tesaglitazar and resveratrol (Figure 8H). Moreover, cardiac SIRT6 protein levels were significantly increased in *db/db* mice treated with tesaglitazar and resveratrol as compared with control *db/db* mice but not to those treated with tesaglitazar alone (Supplemental Figure 10, B and C). On the other hand, SIRT3 protein levels were decreased in *db/db* mice

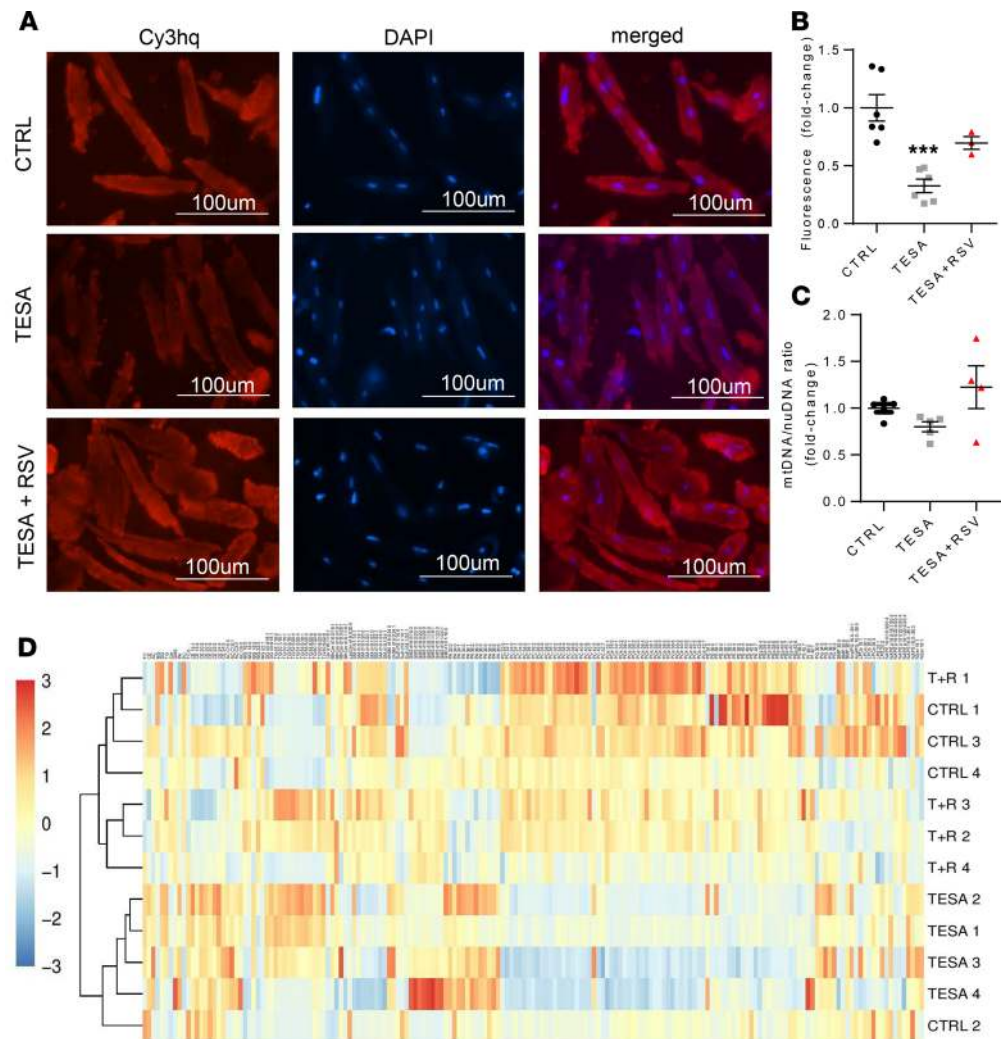


Figure 7. Resveratrol restores mitochondrial function, abundance, and lipid homeostasis in mice treated with tesaglitazar. (A and B) Adult cardiomyocytes (ACMs) were obtained from C57BL/6 mice that were subjected to i.p. daily injections of tesaglitazar (TESA; 2 mg/kg bw) or a combination of tesaglitazar (2 mg/kg bw) and resveratrol (RSV) (100 mg/kg bw) for 7 days. Representative fluorescence microscopy images (A; original magnification, $\times 20$; scale bar: 100 μm) of isolated ACMs stained with MitoTracker Red and quantitation (B) of mitochondrial number/total area (number of analyzed cells, 158 cells from 6 control [CTRL] mice; 157 cells from 6 tesaglitazar-fed mice; 157 cells from 3 mice treated with tesaglitazar and resveratrol [TESA+RSV]). All treatments were performed in 1 experiment. (C) Cardiac mitochondrial DNA (mtDNA) to nuclear DNA (nuDNA) ratio (fold change) in C57BL/6 mice fed with chow diet containing tesaglitazar (0.5 $\mu\text{mol/kg}$ bw) or a combination of tesaglitazar (0.5 $\mu\text{mol/kg}$ bw) and resveratrol (100 mg/kg bw/day) for 6 weeks, ($n = 4-5$). (D) Heatmap and correlation clustering following lipidomic analysis of hearts obtained from C57BL/6 mice fed with chow diet containing tesaglitazar or a combination of tesaglitazar and resveratrol for 6 weeks ($n = 4$). Statistical analyses were performed with 1-way ANOVA followed by Tukey's post hoc correction among groups. *** $P < 0.001$ vs. chow. Error bars represent SEM.

treated with tesaglitazar compared with chow-fed *db/db* mice, but resveratrol supplementation did not correct SIRT3 levels in cardiac tissue of *db/db* mice (Supplemental Figure 10, B and D).

We also treated C57BL/6 mice with high-fat diet (HFD) alone or HFD containing tesaglitazar (0.5 $\mu\text{mol/kg}$ body weight) for 6 weeks. Both mouse groups had similar weight gain rates (Supplemental Figure 10, E and F). Plasma glucose and TGs were significantly lower in mice that were fed with HFD and tesaglitazar compared with control HFD-fed mice (Figure 9, A and B). Tesaglitazar treatment compromised systolic cardiac function (Figure 9, C and D, and Supplemental Table 5). Tesaglitazar treatment also decreased cardiac *PPARGC1a* mRNA (-63%) (Figure 9E) and protein levels (-31%) (Figure 9, F and G) as well as increased Ac-PGC1 α (4.3-fold; Figure 9, F and H). In accordance with the increased Ac-PGC1 α levels, cardiac SIRT1 protein levels were decreased in mice treated with HFD supplemented with tesaglitazar (-61% ; Figure 9, F and I).

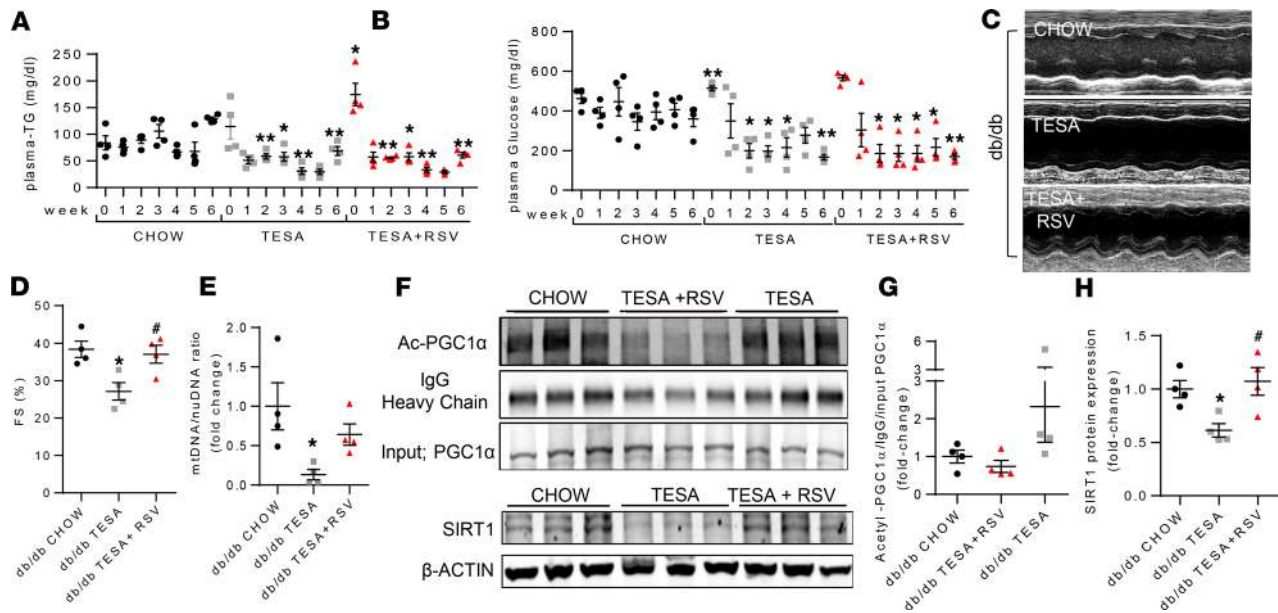


Figure 8. Resveratrol blocks the cardiotoxic effect of tesaglitazar in diabetic mice. Leptin receptor-deficient (*db/db*) mice were treated with regular chow or chow containing either tesaglitazar (TESA; 0.5 $\mu\text{mol}/\text{kg}$ bw) or a combination of tesaglitazar (0.5 $\mu\text{mol}/\text{kg}$ bw) and resveratrol (RSV) (100 mg/kg bw/day) for 6 weeks. Plasma triglycerides (TG) (A) and plasma glucose (B) were determined throughout the treatment. Representative short-axis M-mode images (C), left ventricular fractional shortening (D), and mitochondrial DNA (mtDNA) to nuclear DNA (nuDNA) ratio (fold change) (E) were determined upon termination of the treatment ($n = 4$; data were collected from 1 experiment). Cardiac acetylated-PPAR γ coactivator 1- α (Ac-PGC1 α) normalized to IgG heavy chain, and total PGC1 α , sirtuin 1 (SIRT1), and β -ACTIN immunoblots (F) and densitometric analysis (G and H) of *db/db* mice fed on regular chow, tesaglitazar-containing chow, or chow that contains tesaglitazar and resveratrol diet for 6 weeks ($n = 4$; data were collected from 1 experiment). Statistical analysis was performed with 1-way ANOVA followed by Tukey's post hoc correction. * $P < 0.05$; ** $P < 0.01$ vs. chow; # $P < 0.05$ vs. tesaglitazar. Error bars represent SEM.

Resveratrol abolished its cardioprotective effect in tesaglitazar-treated aMHC-Sirt1^{-/-} mice. We sought to confirm involvement of SIRT1 in mediating the cardioprotective effect of resveratrol in mice treated with tesaglitazar. Therefore, we treated C57BL/6 and *aMHC-Sirt1^{-/-}* mice with chow diet containing a combination of tesaglitazar and resveratrol. Unlike the negation of the toxic effects of tesaglitazar by resveratrol in C57BL/6 mice, the same treatment did not rescue cardiac function in *aMHC-Sirt1^{-/-}* mice (Figure 9, J and K). Thus, cardiomyocyte SIRT1 is crucial in mediating the protective effect of resveratrol.

Discussion

Agonists for PPARs are used to treat hyperglycemia and hypertriglyceridemia in patients with type 2 diabetes. Despite these benefits, some PPAR γ agonists, such as rosiglitazone and pioglitazone, have been associated with increased heart failure due to direct or indirect cardiac effects, such as fluid retention (3). In the last 15 years, potential cardiovascular effects of rosiglitazone have become controversial despite its insulin-sensitizing benefits. Various studies had concluded that TZDs increase risk for heart failure due to direct cardiovascular effects or other indirect effects (5, 6). However, another study acknowledged only a small increase in heart failure incidents in patients on rosiglitazone and simply advised patients and health care providers to be aware of the risks (25). A meta-analysis of randomized trials associated rosiglitazone with increased risk for myocardial infarctions (26). The PROactive study and a meta-analysis of randomized trials showed that although pioglitazone treatment of patients with diabetes increases heart failure incidence, subsequent all-cause mortality is decreased (27, 28). Compared with pioglitazone, rosiglitazone appeared to be associated with a higher risk of heart failure and other cardiovascular events (29). However, the RECORD trial showed that rosiglitazone treatment is associated with an increased risk for heart failure but not for myocardial infarctions, stroke, or cardiovascular mortality (30, 31). A 2010 AHA/ACCF Science Advisory reevaluated the cardiovascular risks of TZDs and concluded that a link between rosiglitazone and heart failure could not be established (32). Thus, in 2013 the FDA removed restrictions on rosiglitazone.

Efforts to discover new PPAR agonists without adverse effects led to the development of dual agonists (glitazars) that activate both PPAR α and PPAR γ , thus combining successfully (4) the lipid-lowering effects of

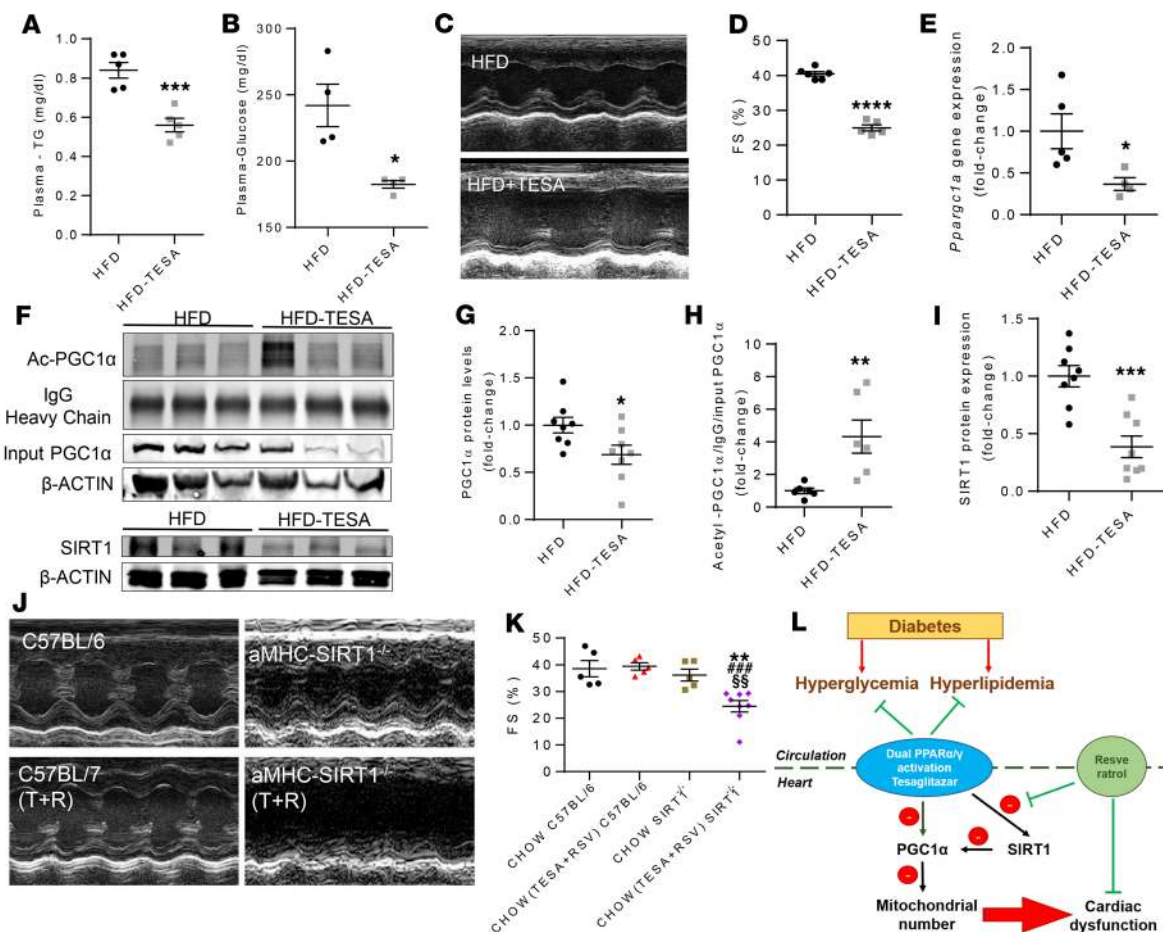


Figure 9. Cardiac SIRT1 ablation abrogates resveratrol beneficial effects in tesaglitazar-mediated cardiac dysfunction. (A–H) C57BL/6 mice fed high-fat diet (HFD) or HFD containing tesaglitazar (0.5 μ mol/kg bw) for 6 weeks (data were collected from 1 experiment). Upon completion of the treatment, plasma triglycerides (TG; **A**) and glucose levels (**B**) were determined. Representative short-axis M-mode images (**C**) and left ventricular fractional shortening (**D**) of C57BL/6 mice fed regular or tesaglitazar-containing HFD for 6 weeks ($n = 5-6$). Cardiac PPAR γ coactivator 1- α (*Ppargc1a*) (**E**; $n = 4-5$) gene expression, acetylated PPAR γ coactivator 1- α (Ac-PGC1 α ; $n = 6$) normalized to IgG heavy chain, and total PGC1 α ($n = 8$), sirtuin 1 (SIRT1; $n = 8$), and β -ACTIN immunoblots (**F**) and their densitometric analysis (**G–I**) from C57BL/6 mice treated with regular or tesaglitazar-containing HFD (0.5 μ mol/kg bw). (**J** and **K**) Representative short-axis M-mode images (**J**) and left ventricular fractional shortening (%) (**K**) of C57BL/6 mice and α myosin heavy chain-SIRT1^{-/-} (aMHC-Sirt1^{-/-}) mice fed regular chow or chow containing a combination of tesaglitazar (0.5 μ mol/kg bw) and resveratrol (RSV; 100 mg/kg bw/d) ($n = 5-8$; data were collected from 2 independent experiments). Statistical analysis for **A–I** was performed with unpaired 2-tailed Student’s *t* tests. Statistical analysis for **K** was performed with 1-way ANOVA followed by Tukey’s post hoc correction. * $P < 0.05$; ** $P < 0.01$; *** $P < 0.001$; **** $P < 0.0001$ vs. HFD (**A–I**) or chow C57BL/6 (**K**). **** $P < 0.001$ vs. tesaglitazar plus RSV C57BL/6. \$\$\$ $P < 0.01$ vs. chow aMHC-Sirt1^{-/-}. Error bars represent SEM. (**L**) Schematic representation of the proposed model. Tesaglitazar treats hyperlipidemia and hyperglycemia but suppresses SIRT1 and PGC1 α , which reduces mitochondrial abundance and causes cardiac dysfunction. The aggravating effect of tesaglitazar on cardiac function is alleviated by coadministration of RSV.

PPAR α with the insulin-sensitizing effects of PPAR γ . Dual PPAR α/γ agonists have various actions, which in several cases deviate between mice and humans. Aleglitazar was protective in mouse cardiomyocytes exposed to high glucose levels in vitro (33) in a PPAR α - and PPAR γ -dependent manner. Another PPAR α/γ agonist, CG301269, also showed beneficial metabolic effects in rodents (34). In the same study, administration of CG301269 in a mouse model of myocardial ischemia/reperfusion did not aggravate further heart failure. In contrast, another dual PPAR α/γ agonist, LY510929, which exerted antihyperlipidemic and antihyperglycemic effects in mice and rats (35), caused left ventricular hypertrophy in rats when was given for 2 weeks (36).

Human studies showed that dual agonists have limited therapeutic benefits. Patients with type 2 diabetes and recent acute coronary syndrome did not show improvement in cardiovascular outcomes when treated with aleglitazar (37). Another dual agonist, saroglitazar, has been approved for clinical use, but there is a precautionary statement for patients with diabetes and congestive heart failure (38). Other glitazars, such as tesaglitazar (5) and muraglitazar (6), were abandoned when clinical trials showed either increased risk for cardiovascular events or other adverse effects. However, the mechanisms that mediate these adverse

outcomes remain unclear. Our study shows that the toxic effect of tesaglitazar, a dual PPAR α / γ agonist, in both healthy C57BL/6 and diabetic *db/db* mice is accounted for by inhibition of both expression and acetylation/deactivation of cardiac PGC1 α . PGC1 α is the transcriptional coactivator of PPARs and controls FAO-related gene expression (39) and mitochondrial biogenesis (14).

PPARs respond to various endogenous ligands, such as steroids, retinoids, cholesterol metabolites, and dietary lipids (10). Upon binding of the ligand, PPARs heterodimerize with retinoid X receptors and bind to cis-acting DNA elements (PPREs) to increase gene transcription. PPARs have broad tissue distribution and promote lipid metabolism in several organs, including the heart (40). FAO is the primary source of cardiac ATP, and its inhibition is associated with cardiac dysfunction (13, 41). While PPAR α promotes FA uptake and FAO (8), PPAR γ increases cardiac lipid accumulation (42). PPAR γ can also induce cardiac FAO-related gene expression (42) when PPAR α is inhibited (11, 13). However, how PPAR α prevents PPAR γ -mediated induction of cardiac FAO, and why combined activation of both PPAR α and PPAR γ causes cardiac dysfunction remained elusive. One given explanation is that combined increase in PPAR γ -driven insulin sensitization and glucose uptake in the setting of higher PPAR α -induced FA metabolism causes combined glucolipotoxicity (43). In the present study, we portray a different explanation, that toxicity by combined PPAR α / γ activation leads to inhibition of SIRT1 and PGC1 α and reduces mitochondrial abundance.

Our previous studies have indicated that combined PPAR α and PPAR γ activation might compromise cardiac function. In those studies, we investigated the cardiac effects of PPAR γ activation (11, 13, 42) and showed that cardiomyocyte-specific overexpression of PPAR γ causes intramyocardial lipid accumulation and cardiac dysfunction (42). We had shown that the observed excessive lipid accumulation may account for some components of cardiac dysfunction, such as β -adrenergic desensitization (13) and arrhythmia (44). Other studies had shown that pharmacologic activation or constitutive cardiomyocyte expression of PPAR α causes cardiac dysfunction (8, 45). However, constitutive PPAR γ expression in cardiomyocytes of *Ppara*^{-/-} mice did not cause cardiac dysfunction, despite increased myocardial lipid content (11), indicating a toxic role for cardiac PPAR α when PPAR γ is activated as well. Moreover, rosiglitazone-mediated PPAR γ activation promotes cardiomyocyte hypertrophy in vitro (46), while fenofibrate-mediated PPAR α activation has the opposite effect in isolated cardiomyocytes and rescues mitochondrial function (47). Activation of PPARs relies on availability of FAs that are released either via LpL-mediated hydrolysis of lipoprotein triglycerides (48) or from intracellular triglycerides via ATGL-mediated lipolysis (49). Thus, cardiac dysfunction in mice that overexpress cardiomyocyte PPAR γ may be partially due to FA-mediated PPAR α activation, which does not occur in aMHC-*Pparg*;*Ppara*^{-/-} mice (11). Tesaglitazar-induced cardiac dysfunction was associated with accumulation of cardiac lipids, including lipids that have been linked with cardiac lipotoxicity, such as acyl-carnitines and diacylglycerols (11, 50). Thus, combined activation of PPAR α and PPAR γ may cause cardiac toxicity due to elevated toxic lipid species. Future studies comparing the cardiovascular effects of treatment with rosiglitazone alone and combined treatment with rosiglitazone and PPAR α antagonists are warranted to elucidate further the mechanism that underlies toxicity by dual activation of PPAR α and PPAR γ . Nevertheless, the controversial findings of clinical studies of TZDs may be due to differential levels of PPAR α activation.

Besides lipotoxicity, our study identified reduced mitochondrial function as another component of cardiac toxicity with tesaglitazar. Activation of PPAR α in mice that were also treated with the PPAR γ agonist, rosiglitazone, prevented rosiglitazone-mediated increase of *Ppargc1a* and FAO-related gene expression and decreased mitochondrial number. Accordingly, we show that pharmacologic or genetic activation of PPAR γ induces *Ppargc1a* expression, which does not occur when both PPAR α and PPAR γ are activated. Moreover, we revealed that both PPAR α and PPAR γ can bind on the -1631/-1609-bp flanking region of the *Ppargc1a* gene promoter and compete for regulating promoter's activity. All the above, are consistent with our previous findings showing that pharmacologic activation of PPAR α in aMHC-*Pparg*^{-/-} mice reduced cardiac expression of *Ppargc1a* and FA metabolism-related genes (11). Similarly, PPAR γ activation in *Ldlr*^{-/-} mice fed with HFD, which increases cardiac PPAR α levels (51, 52), reduces *Ppargc1a* expression and causes cardiac hypertrophy (53). Conversely, we have shown that activation of cardiac PPAR γ in mice with low levels of cardiac PPAR α expression increases *Ppargc1a* expression profoundly (13). Similarly, treatment of *Ppara*^{-/-} mice with tesaglitazar had a milder effect in cardiac function and did not inhibit PGC1 α and SIRT1. Moreover, cardiac dysfunction due to tesaglitazar treatment did not increase expression of genes for cardiac hypertrophy. This suggests that cardiac dysfunction at the early stage of tesaglitazar treatment is an acute effect of the drug that can still be reversed. Tesaglitazar increased *Ppard*, which has also been

involved in the regulation of cardiac FAO (54). Upregulation of cardiac PPAR δ expression correlates with increased expression of UCP3, which is a PPAR δ target gene in cardiac (54) and skeletal muscle (55, 56). Additional studies are needed in order to evaluate potential compensatory activation of PPAR δ upon inhibition of PGC1 α as well as to elucidate whether long-term tesaglitazar treatment causes irreversible cardiac dysfunction and remodeling, accompanied by increased expression of heart failure markers.

Activation of PGC1 α within a critical threshold is crucial for healthy cardiac function. Nevertheless, both reduced and highly increased PGC1 α levels have been associated with cardiac toxicity. More specifically, cardiac PGC1 α expression is decreased in rodents and humans with heart failure (57). Accordingly, *Ppargc1a*^{-/-} mice develop moderate cardiac dysfunction (39), which is aggravated with pressure overload (58). The milder cardiac phenotype at baseline may be accounted for by compensatory function of PGC1 β , which shares functional redundancy with PGC1 α . Indeed, combined knockout of both *Ppargc1a* and *Ppargc1b* inhibits perinatal cardiac mitochondrial biogenesis and causes cardiomyopathy and postpartum death (59). On the other hand, overexpression of cardiomyocyte PGC1 α also causes cardiac dysfunction (14). The cardiotoxic effect of the long-term increase of PGC1 α is associated with impaired mitochondrial biogenesis and function (14). Nevertheless, the same study reported that cardiac function is normal in transgenic lines with lower PGC1 α constitutive expression. Accordingly, short-term PGC1 α overexpression in cultured cardiomyocytes improved mitochondrial biogenesis and oxidative respiration, which has been associated with better cardiac function. Thus, the level of cardiomyocyte PGC1 α activation seems to be critical for determining its protective or aggravating role.

The role of PGC1 α inhibition as a key event that mediates the cardiotoxic effect of dual PPAR α/γ activation is a potentially novel finding. Our data show that dual PPAR α/γ activation reduces both expression and activation of cardiac PGC1 α by enhancing acetylation. In addition, it lowers mitochondrial abundance, which is accompanied by lower OCR in cardiomyocytes. It has been suggested that lower acetylation of cardiac PGC1 α may account for the shift from glycolysis to FAO that occurs during maturation (60). PGC1 α acetylation is controlled by the deacetylase SIRT1 (15), which was reduced in the hearts of mice treated with the dual PPAR α/γ agonist. SIRT1 inhibition has been associated with cardiac dysfunction in various forms of cardiac stress, such as ischemia/reperfusion and cardiac aging (61), whereas young cardiac-specific *Sirt1*^{-/-} mice exhibit normal cardiac function (62). SIRT1 and PGC1 α are activated by resveratrol, which is a polyphenolic compound with antioxidant and antiinflammatory properties (63). The beneficial cardiac effects of resveratrol have been attributed, at least in part, to the activation of SIRT1 (64). Both resveratrol and SIRT1 have been associated with mitochondrial biogenesis (65). Inhibition of SIRT1 has been correlated with diabetes-related cardiometabolic abnormalities, while a protective role has been suggested for activated SIRT1 (66). Resveratrol prevents mitochondrial dysfunction in rats with type 2 diabetes (67, 68). In addition, resveratrol attenuates cardiac injury in rats with type 1 diabetes through SIRT1-mediated regulation of mitochondrial function and PGC1 α deacetylation (69). The mitochondrial SIRT3 is also increased in mice treated with tesaglitazar and resveratrol, although it was not decreased in tesaglitazar-treated mice. The expression of SIRT6 was not altered in any of the groups we tested, except the *db/db* mice that had increased levels upon combined treatment with tesaglitazar and resveratrol. However, as SIRT6 increases PGC1 α acetylation indirectly (70), this change in *db/db* mice cannot explain lower acetylation levels. Thus, SIRT1 seems to be the main isoform with altered expression that may explain increased acetylation of PGC1 α in tesaglitazar-treated mice, which is reversed with combined tesaglitazar and resveratrol treatment. Future studies that will use more SIRT1 activators, such as metformin (71, 72) and SRT1720 (73), are warranted in order to elucidate further the interplay among FAO, altered NAD⁺/NADH ratio, SIRT1, SIRT3, and acetyltransferases, such as GCN5 (74), in regulating acetylation and activation of PGC1 α along with acetylation of mitochondrial proteins.

In summary, our previous (11, 13) and present findings suggest that dual PPAR α/γ -mediated inactivation of the “metabolic network,” which involves SIRT1 and PGC1 α , may account for cardiac toxicity by compromising cardiac mitochondrial biology and energy homeostasis (Figure 9L). Our observations can explain the mechanism that underlies the cardiotoxic effects of one of the dual PPAR α/γ agonists, tesaglitazar. We show for the first time to our knowledge that the negative effects of tesaglitazar can be effectively reversed upon combined administration with resveratrol. Combined treatment with resveratrol and tesaglitazar maintained the beneficial antihyperlipidemic and antihyperglycemic effects of tesaglitazar that were independent from resveratrol, which cannot reduce plasma triglyceride levels (75). Thus, combination of dual PPAR α/γ agonists and activation of the SIRT1-PGC1 α axis holds promise for future therapeutic applications in type 2 diabetes if the same observations are reproduced with other dual PPAR α/γ dual agonists. Moreover, our study provides a guide for design of future PPAR agonists that should be screened for lack of inhibition of PGC1 α activity.

Methods

Chemical reagents. All chemical reagents were obtained from MilliporeSigma unless otherwise noted. Rosiglitazone and WY-14643 were purchased from Enzo Life Sciences.

Animals. Male C57BL/6 (6 weeks old), *db/db* (6 weeks old), and *Ppara*^{-/-} (8 weeks old) mice were obtained from The Jackson Laboratory and fed with chow diet supplemented with tesaglitazar or a combination of tesaglitazar and resveratrol. The *aMHC-Sirt1*^{-/-} (6 weeks old; male) mice have been previously described (76). More information is provided in the Supplemental Methods.

Cells. The human ventricular cardiomyocyte cell line (AC16) (22) was maintained in complete DMEM/F-12 medium at 37°C and 5%CO₂.

Echocardiography analysis. Cardiac function of anesthetized mice was assessed by 2D echocardiography (VisualSonics-Vevo2100) as previously described (12, 77).

Adenoviruses. Recombinant adenoviruses expressing human PPAR γ (Ad-PPAR γ) and control GFP (Ad-GFP) were generated as described previously (78). Adenovirus expressing human PPAR α (Ad-PPAR α) was purchased from Vector Biolabs. Infections of AC16 cells were performed as described previously (78).

Transfection and luciferase assay. FuGENE 6 Transfection Reagent (Promega) was used to transfect AC16 cells, which were seeded in 96-well plates (50,000 cells), with human *PPARGC1A* promoter containing pGL3-BV plasmids according to manufacturer's protocols. More detailed information is included in the Supplemental Methods. Luciferase activity was quantified with the Infinite M1000 PRO plate reader.

Chromatin immunoprecipitation. Heart tissue was cross-linked with formaldehyde. The nuclear fraction was isolated and sonicated to generate a chromatin solution that was then used for immunoprecipitation with anti-PPAR α antibody (Cayman, 101710), anti-PPAR γ (Cell Signaling, 2443), and control IgG (Cell Signaling, 2729). The corrected genomic fragments were validated with quantitative PCR with primers described in Supplemental Table 7.

MitoTracker Red staining. Cells were plated on sterile glass chamber slides and were exposed to MitoTracker Red (Molecular Probes) as we have described previously (79). Description of the procedure and analysis is included in the Supplemental Methods.

Mitochondrial abundance. Mitochondrial abundance was determined by the ratio of mitochondrial copy number (mtDNA) to nuDNA. Both mtDNA and nuDNA were measured by quantitative real-time PCR. For mtDNA we used primers for detecting *CoxII* gene expression and for nuDNA we used primers for *b-globin* (Supplemental Table 7).

RNA purification and gene expression analysis. Total RNA was purified from cells or hearts using the TRIzol reagent (Invitrogen). cDNA synthesis and analysis with SYBR Green Reagent and quantitative real-time PCR were performed as described previously (12). More detailed information is included in the Supplemental Methods.

Protein purification and analysis. Freshly isolated hearts and cells were homogenized in RIPA buffer containing protease/phosphatase inhibitors (Pierce-Biotechnology). Total protein extracts (30–40 μ g) were analyzed with SDS-PAGE and Western Blotting. More detailed information is included in the Supplemental Methods. A complete list of antibodies used can be found in Supplemental Table 6.

Immunoprecipitation. Purified protein lysates (100 μ g) were precleared with protein A/G-agarose beads. The lysates were incubated with antibodies (2 μ g/100 μ g lysate) overnight at 4°C under gentle rotation. More detailed information is included in the Supplemental Methods.

OCR analysis. OCR was determined using a Seahorse Bioscience XF96 Extracellular Flux Analyzer. Primary ACMs isolated from 6-week-old mice were plated (3000 cells/well) in XF96 Seahorse plates. Intact cellular respiration was assayed before and after administration of the mitochondrial inhibitors oligomycin, carbonyl cyanide-p-trifluoromethoxyphenylhydrazone (FCCP), and antimycin A/rotenone. Calculations were made with Wave 2.3 software. More detailed information is included in the Supplemental Methods.

Lipidomic analysis. Lipids were extracted via chloroform-methanol extraction, spiked with appropriate internal standards, and analyzed using a 6490 Triple Quadrupole LC/MS system (Columbia University). A more detailed description is included in the Supplemental Methods.

Statistics. All group comparisons were performed by 1-way ANOVA analysis or by nonpaired 2-tailed Student's *t* test. Multiple comparisons in 1-way ANOVA were assessed using Tukey's post hoc test. Values represent mean \pm SEM. Sample size and *P* values are provided in the figure legends. A *P* value of less than 0.05 was considered significant.

Study approval. All procedures involving animals were approved by the Institutional Animal Care and Use Committees at Temple University and Columbia University.

Author contributions

The research plan was conceived by KD and CK. The methods were performed by CK, IDK, SO, MJL, YY, EAG, YT, WM, AC, DS, and PCS. The analysis of the results was performed by CK, IDK, SO, MJL, YY, EAG, and KD. Experiments were performed by CK, IDK, SO, MJL, YY, EAG, CJP, YT, WM, AC, DS, and MC. Funding was obtained by KD, IJG, and IDK. The original draft was written by CK, IDK, and KD, while CK, IDK, KD, IJG, SO, MJL, YY, EAG, CJP, YT, PCS, MC, JS, and MM reviewed and edited it. Finally, research supervision was conducted by KD and IJG. CK and IDK share first author position for equal contribution in performing experimental procedures as well in writing and editing of the manuscript.

Acknowledgments

Charikleia Kalliora was a MSc student of the “Molecular Basis of Human Diseases” graduate program of the Medical School, University of Crete, Greece. We would like to thank Mesele-Christina Valenti and Brett Brown for technical assistance. This work was supported by National Heart, Lung, and Blood Institute/NIH (NHLBI/NIH) “Pathway to Independence” R00 award HL112853 as well as NHLBI/NIH grant HL130218 and a grant from the W.W. Smith Charitable Trust (to KD). This work was also supported by NHLBI/NIH grants HL073029 and HL135987 (to IJG). IDK was supported by the American Heart Association and the Kahn Family Postdoctoral Fellowship in Cardiovascular Research (18POST34060150).

Address correspondence to: Konstantinos Drosatos, Metabolic Biology Laboratory, Temple University School of Medicine, Center for Translational Medicine, Department of Pharmacology, 3500 North Broad Street, Philadelphia, Pennsylvania 19140, USA. Phone: 215.707.1421; Email: drosatos@temple.edu.

- Fruchart JC. Peroxisome proliferator-activated receptor-alpha (PPARalpha): at the crossroads of obesity, diabetes and cardiovascular disease. *Atherosclerosis*. 2009;205(1):1–8.
- Heikkinen S, Auwerx J, Argmann CA. PPARgamma in human and mouse physiology. *Biochim Biophys Acta*. 2007;1771(8):999–1013.
- Seferović PM, et al. Type 2 diabetes mellitus and heart failure: a position statement from the Heart Failure Association of the European Society of Cardiology. *Eur J Heart Fail*. 2018;20(5):853–872.
- Chatterjee S, Majumder A, Ray S. Observational study of effects of Saroglitazar on glycaemic and lipid parameters on Indian patients with type 2 diabetes. *Sci Rep*. 2015;5:7706.
- Goldstein BJ, Rosenstock J, Anzalone D, Tou C, Ohman KP. Effect of tesaglitazar, a dual PPAR alpha/gamma agonist, on glucose and lipid abnormalities in patients with type 2 diabetes: a 12-week dose-ranging trial. *Curr Med Res Opin*. 2006;22(12):2575–2590.
- Nissen SE, Wolski K, Topol EJ. Effect of muraglitazar on death and major adverse cardiovascular events in patients with type 2 diabetes mellitus. *JAMA*. 2005;294(20):2581–2586.
- Madrazo JA, Kelly DP. The PPAR trio: regulators of myocardial energy metabolism in health and disease. *J Mol Cell Cardiol*. 2008;44(6):968–975.
- Finck BN, et al. The cardiac phenotype induced by PPARalpha overexpression mimics that caused by diabetes mellitus. *J Clin Invest*. 2002;109(1):121–130.
- Park SY, et al. Cardiac-specific overexpression of peroxisome proliferator-activated receptor-alpha causes insulin resistance in heart and liver. *Diabetes*. 2005;54(9):2514–2524.
- Pol CJ, Lieu M, Drosatos K. PPARs: Protectors or opponents of myocardial function? *PPAR Res*. 2015;2015:835985.
- Son NH, et al. PPARγ-induced cardioprototoxicity in mice is ameliorated by PPARα deficiency despite increases in fatty acid oxidation. *J Clin Invest*. 2010;120(10):3443–3454.
- Drosatos K, et al. Cardiac Myocyte KLF5 regulates Ppara expression and cardiac function. *Circ Res*. 2016;118(2):241–253.
- Drosatos K, et al. Peroxisome proliferator-activated receptor-γ activation prevents sepsis-related cardiac dysfunction and mortality in mice. *Circ Heart Fail*. 2013;6(3):550–562.
- Lehman JJ, Barger PM, Kovacs A, Saffitz JE, Medeiros DM, Kelly DP. Peroxisome proliferator-activated receptor gamma coactivator-1 promotes cardiac mitochondrial biogenesis. *J Clin Invest*. 2000;106(7):847–856.
- Rodgers JT, Lerin C, Haas W, Gygi SP, Spiegelman BM, Puigserver P. Nutrient control of glucose homeostasis through a complex of PGC-1alpha and SIRT1. *Nature*. 2005;434(7029):113–118.
- Michan S, Sinclair D. Sirtuins in mammals: insights into their biological function. *Biochem J*. 2007;404(1):1–13.
- Fagerberg B, et al. Tesaglitazar, a novel dual peroxisome proliferator-activated receptor alpha/gamma agonist, dose-dependently improves the metabolic abnormalities associated with insulin resistance in a non-diabetic population. *Diabetologia*. 2005;48(9):1716–1725.
- Bays H, McElhattan J, Bryzinski BS, GALLANT 6 Study Group. A double-blind, randomised trial of tesaglitazar versus pioglitazone in patients with type 2 diabetes mellitus. *Diab Vasc Dis Res*. 2007;4(3):181–193.
- Wallenius K, Kjellstedt A, Thalén P, Löfgren L, Oakes ND. The PPAR α / γ agonist, tesaglitazar, improves insulin mediated

- switching of tissue glucose and free fatty acid utilization in vivo in the obese Zucker rat. *PPAR Res.* 2013;2013:305347.
20. Finck BN, Kelly DP. PGC-1 coactivators: inducible regulators of energy metabolism in health and disease. *J Clin Invest.* 2006;116(3):615–622.
 21. Wu Z, et al. Mechanisms controlling mitochondrial biogenesis and respiration through the thermogenic coactivator PGC-1. *Cell.* 1999;98(1):115–124.
 22. Davidson MM, et al. Novel cell lines derived from adult human ventricular cardiomyocytes. *J Mol Cell Cardiol.* 2005;39(1):133–147.
 23. Ji G, Wang Y, Deng Y, Li X, Jiang Z. Resveratrol ameliorates hepatic steatosis and inflammation in methionine/choline-deficient diet-induced steatohepatitis through regulating autophagy. *Lipids Health Dis.* 2015;14:134.
 24. Sulaiman M, Matta MJ, Sunderesan NR, Gupta MP, Periasamy M, Gupta M. Resveratrol, an activator of SIRT1, upregulates sarcoplasmic calcium ATPase and improves cardiac function in diabetic cardiomyopathy. *Am J Physiol Heart Circ Physiol.* 2010;298(3):H833–H843.
 25. Nesto RW, et al. Thiazolidinedione use, fluid retention, and congestive heart failure: a consensus statement from the American Heart Association and American Diabetes Association. October 7, 2003. *Circulation.* 2003;108(23):2941–2948.
 26. Nissen SE, Wolski K. Effect of rosiglitazone on the risk of myocardial infarction and death from cardiovascular causes. *N Engl J Med.* 2007;356(24):2457–2471.
 27. Erdmann E, et al. Pioglitazone use and heart failure in patients with type 2 diabetes and preexisting cardiovascular disease: data from the PROactive study (PROactive 08). *Diabetes Care.* 2007;30(11):2773–2778.
 28. Lincoff AM, Wolski K, Nicholls SJ, Nissen SE. Pioglitazone and risk of cardiovascular events in patients with type 2 diabetes mellitus: a meta-analysis of randomized trials. *JAMA.* 2007;298(10):1180–1188.
 29. Graham DJ, et al. Risk of acute myocardial infarction, stroke, heart failure, and death in elderly Medicare patients treated with rosiglitazone or pioglitazone. *JAMA.* 2010;304(4):411–418.
 30. Home PD, et al. Rosiglitazone evaluated for cardiovascular outcomes in oral agent combination therapy for type 2 diabetes (RECORD): a multicentre, randomised, open-label trial. *Lancet.* 2009;373(9681):2125–2135.
 31. Mahaffey KW, et al. Results of a reevaluation of cardiovascular outcomes in the RECORD trial. *Am Heart J.* 2013;166(2):240–249.e1.
 32. Kaul S, Bolger AF, Herrington D, Giugliano RP, Eckel RH. Thiazolidinedione drugs and cardiovascular risks: a science advisory from the American Heart Association and American College of Cardiology Foundation. *Circulation.* 2010;121(16):1868–1877.
 33. Chen Y, et al. Alogliptazar, a dual peroxisome proliferator-activated receptor- α and - γ agonist, protects cardiomyocytes against the adverse effects of hyperglycaemia. *Diab Vasc Dis Res.* 2017;14(2):152–162.
 34. Jeong HW, et al. A newly identified CG301269 improves lipid and glucose metabolism without body weight gain through activation of peroxisome proliferator-activated receptor alpha and gamma. *Diabetes.* 2011;60(2):496–506.
 35. Willson TM, et al. The structure-activity relationship between peroxisome proliferator-activated receptor gamma agonism and the antihyperglycemic activity of thiazolidinediones. *J Med Chem.* 1996;39(3):665–668.
 36. Engle SK, et al. Detection of left ventricular hypertrophy in rats administered a peroxisome proliferator-activated receptor alpha/gamma dual agonist using natriuretic peptides and imaging. *Toxicol Sci.* 2010;114(2):183–192.
 37. Lincoff AM, et al. Effect of alogliptazar on cardiovascular outcomes after acute coronary syndrome in patients with type 2 diabetes mellitus: the AleCardio randomized clinical trial. *JAMA.* 2014;311(15):1515–1525.
 38. [No authors listed]. Lipaglyn Product Information. Zydus Discovery. http://lipaglyn.com/downloads/Lipaglyn_Product_Monograph.pdf. Accessed August 29, 2019.
 39. Arany Z, et al. Transcriptional coactivator PGC-1 alpha controls the energy state and contractile function of cardiac muscle. *Cell Metab.* 2005;1(4):259–271.
 40. Auboeuf D, et al. Tissue distribution and quantification of the expression of mRNAs of peroxisome proliferator-activated receptors and liver X receptor-alpha in humans: no alteration in adipose tissue of obese and NIDDM patients. *Diabetes.* 1997;46(8):1319–1327.
 41. Neubauer S. The failing heart—an engine out of fuel. *N Engl J Med.* 2007;356(11):1140–1151.
 42. Son NH, et al. Cardiomyocyte expression of PPARgamma leads to cardiac dysfunction in mice. *J Clin Invest.* 2007;117(10):2791–2801.
 43. Nolan CJ, Ruderman NB, Kahn SE, Pedersen O, Prentki M. Insulin resistance as a physiological defense against metabolic stress: implications for the management of subsets of type 2 diabetes. *Diabetes.* 2015;64(3):673–686.
 44. Morrow JP, et al. Mice with cardiac overexpression of peroxisome proliferator-activated receptor γ have impaired repolarization and spontaneous fatal ventricular arrhythmias. *Circulation.* 2011;124(25):2812–2821.
 45. Zungu M, Young ME, Stanley WC, Essop MF. Chronic treatment with the peroxisome proliferator-activated receptor alpha agonist Wy-14,643 attenuates myocardial respiratory capacity and contractile function. *Mol Cell Biochem.* 2009;330(1-2):55–62.
 46. Pharaon LF, El-Orabi NF, Kunhi M, Al Yacoub N, Awad SM, Poizat C. Rosiglitazone promotes cardiac hypertrophy and alters chromatin remodeling in isolated cardiomyocytes. *Toxicol Lett.* 2017;280:151–158.
 47. Kar D, Bandyopadhyay A. Targeting peroxisome proliferator activated receptor α (PPAR α) for the prevention of mitochondrial impairment and hypertrophy in cardiomyocytes. *Cell Physiol Biochem.* 2018;49(1):245–259.
 48. Ziouzenkova O, et al. Lipolysis of triglyceride-rich lipoproteins generates PPAR ligands: evidence for an antiinflammatory role for lipoprotein lipase. *Proc Natl Acad Sci USA.* 2003;100(5):2730–2735.
 49. Lahey R, Wang X, Carley AN, Lewandowski ED. Dietary fat supply to failing hearts determines dynamic lipid signaling for nuclear receptor activation and oxidation of stored triglyceride. *Circulation.* 2014;130(20):1790–1799.
 50. Drosatos K, et al. Cardiomyocyte lipids impair β -adrenergic receptor function via PKC activation. *Am J Physiol Endocrinol Metab.* 2011;300(3):E489–E499.
 51. Li Y, et al. High-fat feeding in cardiomyocyte-restricted PPARdelta knockout mice leads to cardiac overexpression of lipid metabolic genes but fails to rescue cardiac phenotypes. *J Mol Cell Cardiol.* 2009;47(4):536–543.
 52. Cole MA, et al. On the pivotal role of PPAR α in adaptation of the heart to hypoxia and why fat in the diet increases hypoxic injury. *FASEB J.* 2016;30(8):2684–2697.
 53. Verschuren L, et al. A systems biology approach to understand the pathophysiological mechanisms of cardiac pathological

- hypertrophy associated with rosiglitazone. *BMC Med Genomics*. 2014;7:35.
54. Cheng L, et al. Cardiomyocyte-restricted peroxisome proliferator-activated receptor-delta deletion perturbs myocardial fatty acid oxidation and leads to cardiomyopathy. *Nat Med*. 2004;10(11):1245–1250.
55. Chevillotte E, Rieusset J, Roques M, Desage M, Vidal H. The regulation of uncoupling protein-2 gene expression by omega-6 polyunsaturated fatty acids in human skeletal muscle cells involves multiple pathways, including the nuclear receptor peroxisome proliferator-activated receptor beta. *J Biol Chem*. 2001;276(14):10853–10860.
56. Dressel U, Allen TL, Pippal JB, Rohde PR, Lau P, Muscat GE. The peroxisome proliferator-activated receptor beta/delta agonist, GW501516, regulates the expression of genes involved in lipid catabolism and energy uncoupling in skeletal muscle cells. *Mol Endocrinol*. 2003;17(12):2477–2493.
57. Sihag S, Cresci S, Li AY, Sucharov CC, Lehman JJ. PGC-1alpha and ERRalpha target gene downregulation is a signature of the failing human heart. *J Mol Cell Cardiol*. 2009;46(2):201–212.
58. Arany Z, Novikov M, Chin S, Ma Y, Rosenzweig A, Spiegelman BM. Transverse aortic constriction leads to accelerated heart failure in mice lacking PPAR-gamma coactivator 1alpha. *Proc Natl Acad Sci USA*. 2006;103(26):10086–10091.
59. Lai L, et al. Transcriptional coactivators PGC-1alpha and PGC-1beta control overlapping programs required for perinatal maturation of the heart. *Genes Dev*. 2008;22(14):1948–1961.
60. Fukushima A, et al. Acetylation and succinylation contribute to maturational alterations in energy metabolism in the newborn heart. *Am J Physiol Heart Circ Physiol*. 2016;311(2):H347–H363.
61. Matsushima S, Sadoshima J. The role of sirtuins in cardiac disease. *Am J Physiol Heart Circ Physiol*. 2015;309(9):H1375–H1389.
62. Hsu YJ, et al. Sirtuin 1 protects the aging heart from contractile dysfunction mediated through the inhibition of endoplasmic reticulum stress-mediated apoptosis in cardiac-specific Sirtuin 1 knockout mouse model. *Int J Cardiol*. 2017;228:543–552.
63. Baur JA, Sinclair DA. Therapeutic potential of resveratrol: the in vivo evidence. *Nat Rev Drug Discov*. 2006;5(6):493–506.
64. Lagogue M, et al. Resveratrol improves mitochondrial function and protects against metabolic disease by activating SIRT1 and PGC-1alpha. *Cell*. 2006;127(6):1109–1122.
65. Dolinsky VW, Dyck JR. Experimental studies of the molecular pathways regulated by exercise and resveratrol in heart, skeletal muscle and the vasculature. *Molecules*. 2014;19(9):14919–14947.
66. Winnik S, Auwerx J, Sinclair DA, Matter CM. Protective effects of sirtuins in cardiovascular diseases: from bench to bedside. *Eur Heart J*. 2015;36(48):3404–3412.
67. Beaudoin MS, et al. Impairments in mitochondrial palmitoyl-CoA respiratory kinetics that precede development of diabetic cardiomyopathy are prevented by resveratrol in ZDF rats. *J Physiol (Lond)*. 2014;592(12):2519–2533.
68. Cao MM, Lu X, Liu GD, Su Y, Li YB, Zhou J. Resveratrol attenuates type 2 diabetes mellitus by mediating mitochondrial biogenesis and lipid metabolism via sirtuin type 1. *Exp Ther Med*. 2018;15(1):576–584.
69. Fang WJ, Wang CJ, He Y, Zhou YL, Peng XD, Liu SK. Resveratrol alleviates diabetic cardiomyopathy in rats by improving mitochondrial function through PGC-1 α deacetylation. *Acta Pharmacol Sin*. 2018;39(1):59–73.
70. Dominy JE, et al. The deacetylase Sirt6 activates the acetyltransferase GCN5 and suppresses hepatic gluconeogenesis. *Mol Cell*. 2012;48(6):900–913.
71. Lu JQ. Traditional Chinese medical theory and human circadian rhythm in the occurrence of ischemic stroke. *Stroke*. 1991;22(10):1329.
72. Caton PW, Nayuni NK, Kieswich J, Khan NQ, Yaqoob MM, Corder R. Metformin suppresses hepatic gluconeogenesis through induction of SIRT1 and GCN5. *J Endocrinol*. 2010;205(1):97–106.
73. Milne JC, et al. Small molecule activators of SIRT1 as therapeutics for the treatment of type 2 diabetes. *Nature*. 2007;450(7170):712–716.
74. Lerin C, Rodgers JT, Kalume DE, Kim SH, Pandey A, Puigserver P. GCN5 acetyltransferase complex controls glucose metabolism through transcriptional repression of PGC-1alpha. *Cell Metab*. 2006;3(6):429–438.
75. Dash S, Xiao C, Morgantini C, Szeto L, Lewis GF. High-dose resveratrol treatment for 2 weeks inhibits intestinal and hepatic lipoprotein production in overweight/obese men. *Arterioscler Thromb Vasc Biol*. 2013;33(12):2895–2901.
76. Hsu CP, et al. Silent information regulator 1 protects the heart from ischemia/reperfusion. *Circulation*. 2010;122(21):2170–2182.
77. Hoffman M, et al. Myocardial strain and cardiac output are preferable measurements for cardiac dysfunction and can predict mortality in septic mice. *J Am Heart Assoc*. 2019;8(10):e012260.
78. Bosma M, et al. Sequestration of fatty acids in triglycerides prevents endoplasmic reticulum stress in an in vitro model of cardiomyocyte lipotoxicity. *Biochim Biophys Acta*. 2014;1841(12):1648–1655.
79. Kokkinaki D, et al. Chemically synthesized Secoisolariciresinol diglucoside (LGM2605) improves mitochondrial function in cardiac myocytes and alleviates septic cardiomyopathy. *J Mol Cell Cardiol*. 2019;127:232–245.